Title

A nutrient-specific gut hormone arbitrates between courtship and feeding

Journal

Nature, 602(7898)

ISSN

0028-0836

Authors

Lin, Hui-Hao

Kuang, Meihua Christina

Hossain, Imran

et al.

Publication Date

2022-02-24

DOI

10.1038/s41586-022-04408-7

Peer reviewed

Published in final edited form as:

Nature. 2022 February ; 602(7898): 632–638. doi:10.1038/s41586-022-04408-7.

A nutrient-specific gut hormone arbitrates between courtship and feeding

Hui-Hao Lin[1], **Meihua Christina Kuang**[1], **Imran Hossain**[1,2], **Yinan Xuan**[1], **Laura Beebe**[1], **Andrew K. Shepherd**[1], **Marco Rolandi**[2], **Jing W. Wang**[1,#]

[1]Neurobiology Section, Division of Biological Sciences, University of California San Diego, La Jolla, CA 92093, USA

[2]Department of Electrical and Computer Engineering, University of California Santa Cruz, Santa Cruz, CA 95064, USA

SUMMARY

Animals must set behavioral priority in a context-dependent manner and switch from one behavior to another at the appropriate moment. Here we probe the molecular and neuronal mechanisms that orchestrate the transition from feeding to courtship in *Drosophila*. We find that feeding is prioritized over courtship in starved males, and the consumption of protein-rich food rapidly reverses this order within a few minutes. At the molecular level, a gut-derived, nutrient-specific neuropeptide hormone — Diuretic hormone 31 (Dh31) — is both necessary and sufficient to induce a switch from feeding to courtship. We further address the underlying kinetics with calcium imaging experiments. Amino acids from food acutely activate $Dh31^+$ enteroendocrine cells in the gut, elevating Dh31 levels in circulation. In addition, three-photon functional imaging of intact flies shows that optogenetic stimulation of $Dh31^+$ enteroendocrine cells rapidly excites a subset of brain neurons that express Dh31 receptor (Dh31R). Gut-derived Dh31 excites the brain neurons through the circulatory system within a few minutes, a speed in line with the feeding-courtship behavioral switch. At the circuit level, there are two distinct populations of $Dh31R^+$ neurons in the brain, with one population inhibiting feeding through allatostatin-C and the other promoting courtship through corazonin. Together, our findings illustrate an elegant mechanism by which the consumption of protein-rich food triggers the release of a gut hormone which in turn prioritizes courtship over feeding through two distinct pathways.

Keywords

Nutrient; enteroendocrine; gut-brain axis; neuropeptide; courtship; corazonin; GnRH; CGRP; three-photon microscopy

[#]Corresponding: jw800@ucsd.edu.

AUTHOR CONTRIBUTIONS

Conceptualization, H.-H.L., M.C.K., I.H., Y.X., J.W.W.; Methodology, H.-H.L., M.C.K., I.M., Y.X., J.W.W.; Investigation, H.-H.L., M.C.K., I.M., Y.X., L.B., A.K.S., J.W.W.; Writing-Original Draft, -H.H.L., M.C.K., I.M., Y.X.; Writing-Review and Editing, H.-H.L., M.C.K., I.M., Y.X., L.B., A.K.S., M.R., J.W.W.; Funding Acquisition, H.-H.L., M.R., J.W.W.; Resources, H.-H.L., M.R., J.W.W.; Supervision, J.W.W.

DECLARATION OF INTERESTS

The authors declare no competing interests.

MAIN

Animals typically display one behavior at a time[1]; they must have mechanisms to set behavioral priority and switch from one behavior to another at the appropriate moment[2]. Adaptive prioritization between feeding and courtship in particular is critical for the maximization of evolutionary fitness[3,4]. For example, excessive time spent on feeding could lead to a loss of reproductive opportunity while insufficient feeding may reduce reproductive output, thereby lowering evolutionary fitness. To understand how animals set behavioral priority, it is imperative to study the interaction between the relevant motivational systems[5]. However, most studies focus on individual systems that regulate feeding[6–9] and courtship[10–15]. Here, we investigate the context that determines the priority between feeding and courtship, and address the molecular and neuronal mechanisms that allow for a transition from feeding to courtship in *Drosophila*.

Ingestion of amino acids rapidly prioritizes courtship over feeding

We devised an assay to monitor the behavior of individual male flies towards food and mate (Fig. 1a). With this feeding-courtship assay, we found that fed males spent little or no time on feeding and most time on courting the virgin female in an observation period of 30 min (Fig. 1b). By contrast, 24-hr starved males delayed their courtship by a few minutes until they had consumed yeast, a protein-rich food. This result indicates that feeding is prioritized over courtship in starved males and food consumption rapidly reverses this order.

We asked which macronutrient in food is required for the switch from feeding to courtship. Since protein influences the reproductive success of male flies more than carbohydrates[16], we prepared food containing amino acids or sucrose of various concentrations (Supplementary Tables 1 and 2) by modifying a defined *Drosophila* food recipe[17]. After consuming sucrose, males did not switch from feeding to courtship, even though flies spent less time feeding when the sucrose concentration was higher (Fig. 1c). By contrast, starved males transitioned from feeding to courtship when the food contained amino acids (Fig. 1d). The feeding duration was prolonged when the food contained a lower concentration of amino acids or the males had been starved for a longer period. This result suggests that specific nutrients rather than their caloric content promote courtship behavior in male flies.

To identify a signaling molecule for this nutrient-dependent behavioral switch, we turned to an established high-throughput two-male courtship assay[18]. We first verified that the two-male courtship assay is capable of detecting the courtship promoting effect of amino acids. We fed two genetically identical males with different foods and placed them together with one virgin female (Fig. 1e). During the 2-hr observation period, 74% of the males fed with amino acids (200 mM biologically available nitrogen) copulated with the female, whereas only 26% of the males fed with nutrient-less agar did so (Fig. 1f). By contrast, the males fed with sucrose (50 mM) exhibited a copulation rate similar to those fed with agar. Consistent with the observation from the feeding-courtship assay, amino acids — but not sucrose — have an aphrodisiac effect on males. We next fed one male with amino acids and the other one with sucrose at isocaloric concentrations. Again, males fed with amino acids

(200 mM) exhibited a higher copulation rate than their counterparts fed with sucrose (50 mM).

Next, we carried out experiments to identify nutrient-dependent signaling molecules that promote male courtship. It has been suggested that some satiety hormones promote reproductive behaviors in mammals[19]. Satiety hormones, such as cholecystokinin (CCK) and glucagon-like peptide 1 (GLP1), are released by enteroendocrine cells in the gastrointestinal (GI) tract in mammals[6]. Similarly, *Drosophila* enteroendocrine cells express an array of neuropeptide hormones[20–22]. Interestingly, intake of amino acids can elevate calcium levels in Dh31$^+$ enteroendocrine cells in *Drosophila*[23]. We therefore explored whether Dh31 is required for the aphrodisiac effect of amino acids. Indeed, when both competing males carried a *Dh31* mutation[24], the ingestion of amino acids no longer increased copulation rate (Fig. 1f). We then generated a mutation of the Dh31 receptor gene (*Dh31R*) using CRISPR/Cas9 genome editing (Extended Data Fig. 1). This mutation also abolished the effect of amino acids (Fig. 1f). Thus, Dh31 signaling is required for the aphrodisiac effect of amino acids.

Gut-derived Dh31 promotes male courtship through Dh31R$^+$ Crz$^+$ neurons in the brain

Dh31 is widely expressed in adult flies, including neurons in the brain and ventral nerve cord (VNC) as well as enteroendocrine cells in the GI tract (Extended Data Fig. 2a). In an effort to identify the source of Dh31 responsible for the aphrodisiac effect of amino acids, we generated a knock-in GAL4 line to visualize the expression pattern of the Dh31 gene (Extended Data Fig. 1) and validated it with an antiserum against Dh31. We found that *Dh31$^{T2A\text{-}GAL4}$* labels 84%, 88% and 98% of Dh31$^+$ cells in the brain, VNC and midgut, respectively (Extended Data Fig. 2a). Importantly, RNAi-mediated *Dh31* knockdown driven by *Dh31$^{T2A\text{-}GAL4}$* abolished the effect of amino acids on courtship (Extended Data Fig. 2b), recapitulating the phenotype of the *Dh31* mutation (Fig. 1f), thereby validating the utility of the genetic reagents.

Is Dh31 expression in the gut required for the courtship effect of amino acid intake? We next selectively knocked down *Dh31* inside and outside the brain by taking advantage of the transgene *otd-nls::flp* that expresses FLP only in the brain[25]. We found that the aphrodisiac effect of amino acids is intact in flies with *Dh31* knockdown in the brain, but abolished in those with *Dh31* knockdown outside the brain (Extended Data Fig. 2c, d). We then targeted Dh31$^+$ cells in the midgut by suppressing the GAL4 function of *Dh31-GAL4*[26,27] with *Tsh-GAL80*[28] (Fig. 2a). For these gut-specific *Dh31* knockdown flies (Extended Data Fig. 3a, b), ingestion of amino acids did not increase copulation rate (Extended Data Fig. 3c), suggesting that Dh31 expression in enteroendocrine cells is required for the effect of amino acids. We then asked whether activation of Dh31$^+$ enteroendocrine cells is sufficient to promote male courtship. We ectopically expressed the mammalian capsaicin receptor (VR1), a ligand-gated cation channel of the TRP family[29,30], in Dh31$^+$ enteroendocrine cells. Indeed, males fed with a mixture of capsaicin and sucrose had higher copulation rates than those fed with sucrose alone (Extended Data Fig. 3c). Thus, Dh31 signaling from the gut is both necessary and sufficient for the promotion of courtship by ingested amino acids.

We next searched for the neural target of Dh31 for the aphrodisiac effect of amino acids. It has been reported that Dh31R is expressed in 7 pairs of corazonin (Crz) neurons in the adult brain[31], which we confirmed (Fig. 2d). We found that RNAi-mediated knockdown of *Dh31R* in Crz neurons abolished the courtship effect of amino acids (Extended Data Fig. 4a, b). However, the *Crz-GAL4* line we used for *Dh31R* knockdown labels other neurons in the VNC in addition to the Crz^+ neurons in the brain (Extended Data Fig. 4). To narrow down the $Dh31R^+$ Crz^+ neurons that mediate the aphrodisiac effect of amino acids, we used a similar genetic strategy as described earlier (Extended Data Fig. 2) to knock down *Dh31R* in Crz^+ neurons in the brain or VNC. *Dh31R* knockdown in Crz^+ neurons in the brain, but not the VNC, abolished the effect of amino acids on courtship (Extended Data Fig. 4c, d). Corroborating this result, *Crz* knockdown selectively in the brain, but not in the VNC, abolished the effect of amino acids (Extended Data Fig. 5). These results indicate that Dh31R expression in the brain Crz^+ neurons is necessary for the aphrodisiac effect of dietary amino acids.

We then determined whether Dh31 signaling in the gut-brain axis is required for the re-ordering of feeding and courtship behavior by amino acid feeding, using the feeding-courtship assay. When *Dh31* was knocked down in the gut, starved males continued to feed without switching to courtship, and even ad libitum-fed males displayed dramatically reduced courtship activity (Fig. 2b and Extended Data Fig. 6a, b). Conversely, chemogenetic activation of gut $Dh31^+$ cells conferred a transition, causing males to court females after feeding on food containing the ligand capsaicin (Fig. 2c and Extended Data Fig. 6c). Furthermore, *Dh31R* knockdown in brain Crz^+ neurons also abolished the switch from feeding to courtship (Fig. 2e and Extended Data Fig. 6d).

Amino acids increase the level of circulating Dh31 via activating enteroendocrine cells

Do $Dh31^+$ enteroendocrine cells respond to amino acids? We developed an *ex vivo* midgut preparation for calcium imaging and used $Dh31^{T2A\text{-}GAL4}$ to drive the expression of GCaMP7c, a genetically encoded calcium indicator[32] (Fig. 3a). On average, we obtained nutrient-triggered responses from 48±3 (mean ± SEM, n = 11) healthy $Dh31^{T2A\text{-}GAL4}$ cells from each male. We found that $Dh31^{T2A\text{-}GAL4}$ enteroendocrine cells respond to both essential and nonessential amino acids, but not to glucose or fructose (Extended Data Fig. 7a). Overall, the number of activated cells increased with the concentration of amino acids (Fig. 3b, d). For each responding cell, the intensity of calcium activity increased with the stimulation concentration (Fig. 3b and Extended Data Fig. 7b). The average GCaMP signal exhibited a dosage curve that saturates at about 100 mM (Fig. 3c, e).

We next asked whether feeding flies with amino acids increases the level of Dh31 in the circulatory system. Our western blot experiments show that a Dh31 band was detected in the hemolymph of wild-type males, but not in the *Dh31* mutant males (Fig. 3f). Importantly, the Dh31 level was higher in male flies fed with amino acids than that of males fed with sucrose. Furthermore, for males fed with amino acids, gut-specific *Dh31* knockdown reduced Dh31 level. The ingestion of capsaicin also increased Dh31 level in the hemolymph of males that expressed VR1 in the gut $Dh31^+$ cells. Taken together, results from our

calcium imaging and western blot experiments indicate that ingested amino acids activate $Dh31^+$ enteroendocrine cells, causing them to release Dh31 into circulation.

Gut-derived Dh31 activates $Dh31R^+$ neurons in the brain through circulation

To address how gut-derived Dh31 influences the activity of Crz^+ neurons in the brain, we took advantage of a non-invasive imaging system that preserves the circulatory system[33]. Specifically, three-photon microscopy was used to image calcium activity of brain Crz^+ neurons through the cuticle of an intact fly (Fig. 3g). We used Crz^{LexA} (Extended Data Fig. 1c) to express GCaMP7s in Crz^+ neurons. Indeed, these neurons exhibited calcium activity in response to Dh31 injected into the circulatory system through the heart tube of male flies. We next asked whether activation of $Dh31^+$ cells in the gut can elicit calcium activity in the brain Crz^+ neurons. We expressed CsCrimson[34] in Dh31 enteroendocrine cells with the *Dh31-GAL4* driver. We found that the brain Crz^+ neurons exhibited robust calcium activity in response to optogenetic activation of $Dh31^+$ cells in the gut (Fig. 3h). Notably, the response latency decreased from 18 to 3 min with increasing light intensity, whereas peak ΔF/F did not change with stimulation intensity.

If gut-derived Dh31 reaches the brain through the circulatory system rather than a fast-synaptic connection between the GI tract and the brain, retarding circulation by cardiac arrest should increase the response latency of Crz^+ neurons in the brain. A brief exposure to CO_2 has been shown to cause cardiac arrest in flies[35]. We validated this and found that flooding our imaging chamber with CO_2 stopped the heart briefly and heartbeat frequency returned to the normal level in about 5 min (Extended Data Fig. 8a). We observed an increase of about 7 min in the response latency of the Crz^+ neurons when optogenetic activation of $Dh31^+$ enteroendocrine cells occurred under the influence of CO_2 (Fig. 3i). Again, ΔF/F was not changed by CO_2 exposure (Extended Data Fig. 8b). We next asked whether the intake of amino acids activates brain Crz^+ neurons through Dh31 signaling. Using CaLexA, a calcium sensor that drives GFP expression in response to sustained cytosolic calcium[36], we found that flies fed with amino acids had higher GFP levels in the brain Crz^+ neurons than those fed with sucrose (Fig. 3j). And cell autonomous expression of Dh31R was required for the higher GFP expression in flies fed with amino acids. Taken together, results from our three-photon imaging and CaLexA experiments suggest that Dh31 released from enteroendocrine cells activates the Crz^+ neurons in the brain through the circulatory system.

Gut-derived Dh31 suppresses protein feeding through $Dh31R^+$ $AstC^+$ neurons in the brain

Our results suggest that Dh31 released from the gut has opposing effects on feeding and courtship (Fig. 2b). While it promotes courtship by activating $Dh31R^+$ Crz^+ neurons in the brain (Fig. 2e), *Dh31R* knockdown in brain Crz^+ neurons did not increase feeding duration (Fig. 2e and Extended Data Fig. 6d). We therefore performed a genetic screen to search for other $Dh31R^+$ neurons that suppress feeding. To measure food intake, we adopted a dye-based method called EX-Q, in which the dye contents of the excreta from a group of flies are quantified by spectrophotometry to determine the volume of food they consume[37]. We found that males with *Dh31* knockdown in the gut consumed more amino acids than control males in 24 hrs (Fig. 4a). By contrast, control and knockdown males consumed

similar amounts of sucrose. We therefore concluded that gut Dh31 is a satiety signal that regulates amino acid intake. *Dh31R* knockdown in brain Crz^+ neurons, however, did not affect food intake (Fig. 4b), suggesting another population of neurons respond to the Dh31 signal to suppress protein intake.

Neuropeptides such as Ion transport peptide (Itp), Allatostatin A (AstA), Leucokinin (Lk), Drosulfakinin (Dsk), Proctolin (Proc), Allatostatin B (AstB), Bursicon-α (Burs- α), Neuropeptide F (Npf), Allatostatin C (AstC) are required for normal feeding or the release of metabolic hormones[26,38–45]. We therefore investigated whether brain neurons expressing these neuropeptides also express Dh31R and whether *Dh31R* knockdown in these neurons increases the intake of amino acids. We found that Dh31R is expressed in AstA, AstC, Lk, and Dsk neurons (Extended Data Fig. 9a). However, amino acid intake was increased only when *Dh31R* was knocked down in $AstC^+$ neurons (Extended Data Fig. 9b). We identified a driver line, *R67F03-GAL4*[46], that captures a majority of the brain $AstC^+$ neurons, which express Dh31R but not Crz (Fig. 4c). Brain-specific knockdown of *Dh31R* or *AstC* by intersecting this driver line with *otd-nls::flp*, as validated before (Extended Data Fig. 2), increased the intake of amino acids, but not sucrose (Fig. 4d, e). Conversely, knockdown of *Dh31R* or *AstC* in *R67F03* neurons outside the brain did not change the intake of either amino acids or sucrose (Extended Data Fig. 9e). Thus, we have identified two different populations of $Dh31R^+$ neurons in the brain, with one population releasing Crz to promote courtship and another releasing AstC to suppress protein feeding (Fig. 4f).

DISCUSSIONS

How do animals select one behavior over others in an environment cluttered with multitudes of sensory stimuli? Abraham Maslow suggested that human needs are organized as a pyramid[47]. When physiological needs are met, social needs will be prioritized. This theory offers an elegant logic to explain the prioritization of animal behaviors as well as the circumstances under which an animal would transition from one behavior to another[5,48]. Here, we provide a neural and molecular basis for the transition from feeding to courtship. Our study reveals that circulating neuropeptide Dh31, released from the GI tract by ingested amino acids, excites $Dh31R^+$ neurons in the *Drosophila* brain. One population of $Dh31R^+$ neurons releases corazonin to promote courtship while another population enlists AstC to suppress feeding. Concerted regulation of these two circuits directs behavioral selection in response to a shift in nutritional status.

Our study identifies amino acids as nutrients that promote male courtship. Dietary protein is also a key factor in limiting reproductive output[16,49]. Regulation by the same nutrient ensures a coordination between reproductive behavior and physiology. Furthermore, corazonin, an ortholog of gonadotropin-releasing hormone (GnRH)[50], serves as a downstream signal in the circuit for courtship promotion. In musk shrews, GnRH can reverse the effect of food restriction on female sexual receptivity[51]. Thus, it appears that metabolic cues target a similar molecular mechanism to regulate mating behavior in diverse animal species.

Our study shows that the *Drosophila* GI tract conveys the availability of amino acids to the brain through circulatory Dh31. In general, the GI tract has immediate access to digested food content, enabling it to provide fast, anticipatory nutritional signals[52,53]. In this context, Dh31 serves as a feedforward signal to report the immediate availability of amino acids. A previous study showed that calcitonin gene-related peptide (CGRP) is an anorexigenic neuropeptide that suppresses feeding in a feedforward circuit[54]. Our study shows that Dh31, an analog of CGRP[31], suppresses the intake of protein food, suggesting that Dh31 serves a conserved function in feeding regulation.

Neuropeptides are known to play an important role in the orderly transition between different behaviors. For instance, mammals typically transition from wakefulness to non-REM sleep rather than directly to REM sleep. The neuropeptide orexin is required for the orderly transition between these wake-sleep states[55]. Orexin excites the monoaminergic neurons, which activate REM-off neurons and simultaneously inhibit REM-on neurons. Individuals with narcolepsy can enter REM sleep directly from the waking state due to a loss of orexin signaling. Similarly, our study shows that Dh31 is a neuropeptide required for the transition from feeding to courtship in *Drosophila*. In the absence of Dh31, male flies fail to enter the courtship state even after they stop feeding.

Dh31 ultimately acts on the brain $Dh31R^+$ neurons to arbitrate between two behaviors: feeding and courtship. These neurons can therefore be considered a neural arbitrating node. The previously identified ISN neurons control drinking and feeding in *Drosophila*[56]. Activity of the ISN neurons, increased by hunger and decreased by dehydration, promotes feeding and suppresses water drinking. Thus, the ISN neurons function as an arbitrating node. In yet another example, a pair of glucose-sensing neurons in the fly brain promote insulin release while simultaneously suppressing AKH release[57], providing a transition from one satiety state to another. This kind of node is reminiscent of the spinal stretch reflex circuitry that coordinates muscle activity of a single joint. Sensory signaling from the stretched muscle excites motor neurons of the synergistic muscles and inhibits motor neurons of the antagonistic muscles. Unlike the stretch reflex circuit that uses small neurotransmitters for transient activation, $Dh31R^+$ neurons release neuropeptides (AstC and corazonin) to regulate behaviors. Activation of neuropeptide receptors can generate long-lasting changes in behavioral state. For example, *C. elegans* worms alternate between dwelling and roaming during foraging, which are regulated by serotonin and PDF, respectively[58]. After a rapid transition, worms maintain a long-lasting state of dwelling or roaming.

In our circuit model for the hierarchy of needs, arbitrating nodes are the elementary circuits that are modulated by metabolic fuels, hormones and neuropeptides, in response to external and internal stimuli. Coupling gut imaging with three-photon brain imaging provides an opportunity to study how neuropeptides released outside the brain reconfigure neural arbitrating nodes in the brain in real time for behavioral prioritization.

METHODS

Generation of transgenic flies

The knock-in lines were generated as described previously[59] with some modifications. In brief, gRNA sequences of target genes for each knock-in line were cloned into the U6 promoter plasmid. For the *Dh31*$^{T2A\text{-}Gal4}$ knock-in line, a T2A-Gal4.2-RFP cassette containing T2A-GAL4.2, two LoxP sites, 3XP3-RFP, βtub50d-3'UTR and two homology arms was cloned into the pUC57-Kan vector as a donor template for repair. For the two LexA knock-in lines (*Dh31R*^{LexA} and *Crz*^{LexA}), an nls-LexA::p65 cassette containing nls-LexA::p65, two loxP sites, 3XP3-RFP and two homology arms was cloned into the pUC57-Kan vector as a donor template for repair. For all knock-in lines, gRNAs and hs-Cas9 were supplied in DNA plasmids, together with the donor plasmids for microinjection into embryos of control strain *w*^{1118}. F1 flies carrying the selection marker 3xP3-RFP were validated by genomic PCR and sequencing. For the *Dh31*$^{T2A\text{-}Gal4}$ knock-in line, the T2A-Gal4.2-RFP cassette was inserted at the C-terminus of *Dh31*/CG13094. For the two LexA knockin lines, CRISPR strategy generated a deletion: a 25-bp deletion in *Dh31R*/CG32843 and a 47-bp deletion in *Crz*/CG3302 (Supplementary Table 5). In each case, the deletion was replaced by the nls-LexA::p65-LoxP-3xP3-RFP-LoxP cassette. CRISPR-mediated mutagenesis was performed by WellGenetics (Taipei City, Taiwan).

Dh31-T2A-GAL4.2 gRNA sequence: CATCCAGACGCCTTAGACATCGG

Dh31R-LexA::p65 gRNA sequence: CTGGTCGCTCATGGTCGTCGTGG

Crz-LexA::p65 gRNA sequence: TGCACATGGAGAGCGTGAAGAGG

Fly husbandry

Flies were raised on standard fly food (containing yeast, cornmeal, agar and molasses) at 25°C in a 12:12 light-dark cycle. Experimental flies were collected at eclosion as naïve males and virgin females and raised in same sex groups of 10 per vial. For optogenetic experiments, flies were raised on fly food containing all-trans-retinal (0.4 mM) in the dark for 7 days and starved for 24 hr before the experiment. For CaLexA experiments, naive males were raised in groups of 10 per vial with food containing either a mixture of 20 amino acids (200 mM) or sucrose (50 mM) in 2% agar for 5 days. All experimental flies were flipped to fresh vials every two days.

Behavioral assays

(1) Feeding-courtship assay—Behavioral chambers were constructed using 35 mm petri dishes. The base of each petri dish was filled with silicon (Sylgard 184) to create a space 5 mm in height when covered. Before the experiment, a food patch containing different nutrients in 1% agar - either yeast (2.5%), an amino acid mixture (200 mM), sucrose (50 mM) or a sucrose/capsaicin mixture (50 mM sucrose and 50 μM capsaicin) was placed at the center of the behavioral chamber on an 18mm circle cover glass. One 7-day old naïve male of a given genotype and one 2-day old virgin Canton-S female were tested. Under normal room light, feeding behavior (proboscis extension on the food patch) and courtship behaviors (orienting, tapping, chasing, wing extension, licking, attempted

copulation and copulation success) were recorded for 30 min at a frame rate of 20 Hz. The video frame rate was converted to 1 Hz and behavior was manually analyzed post hoc.

(2) Two-male courtship assay—Two-male courtship assays were performed as previously described[18] with 7-day old males and 2-day old virgin females. Before the assay, starved male flies were fed with an amino acid, sucrose or control agar diet for one hour. See Supplementary Tables 1 and 3 for food recipes, modified from the holidic medium[17]. A red food dye (Market Pantry) was added at 0.4% (v/v) for consumption visualization. A majority of male flies consumed food during the 1-hr feeding period. Male flies without the food coloration in their abdomen were excluded from experiments. Two naïve males fed with different diets were paired with one virgin female. The identity of the male to first copulate with the female and the copulation latency were manually recorded during a 2-hour observation period. Courtship chambers in which neither male copulated with the female during the 2-hour period were excluded from further analysis. To distinguish between the two competing males, one of the two males was dusted with a fluorescent dye (UVXPBR, LDP LLC) 48 hours prior to the experiment. Dye application was alternated between the two diet conditions to minimize any possible dye-induced behavioral bias. Copulation percentage was calculated by dividing the number of first copulations by males fed with one diet by the total number of first copulations.

(3) EX-Q feeding assay—The excreta quantification experimental protocol was performed as previously described[37]. Briefly, ten 7-day old naïve male flies were transferred to a standard fly vial (Genesee Scientific, catalog # 32–116) with a 5.5 mm diameter food cup at the bottom of the vial. Amino acid (200 mM) and sucrose (50 mM) diets were prepared as in Supplementary Tables 1 and 2, supplemented with 0.25% erioglaucine disodium salt (Sigma) as dye for quantification. Flies in groups of 10 were allowed to feed on the dye-containing food for 24 hrs before being fed with a yeast (2.5%) and sucrose (2.5%) mixture without dye for 4 hours to allow for all dye-containing food to be excreted. To quantify food intake, dye-containing excreta from each vial was dissolved in distilled water and dye concentration was measured with a spectrophotometer (DU-730, Beckman-Coulter). Absorbance at 630 nm was converted to food volume consumed according to a standard curve.

Immunofluorescence

Fly tissue samples (brain, VNC and gut) were dissected in phosphate-buffered saline (PBS). Samples were fixed in 4% paraformaldehyde with 7% picric acid at room temperature for 30 min. Samples were transferred to PBS containing 0.5% Triton X-100 and 10% normal goat serum, and degassed in a vacuum chamber for six cycles (10 min/cycle) to expel tracheal air. Next, samples were transferred into new PBS containing 0.5 % Triton X-100 and 10% normal goat serum and kept at room temperature for 2 hrs. For immunostaining, samples were kept at 4°C for 48 hrs in PBS containing 0.5% Triton X-100, 10% normal goat serum, and a primary antibody. Primary antibodies included: mouse nc82 antibody at 1:50 dilution (Developmental Studies Hybridoma Bank, University of Iowa), anti-Dh31 at 1:500 dilution, anti-Crz, anti-AstB, anti-AstC[60], anti-Bursicon[61], anti-Npf (RayBiotech) and anti-Dh31R[62] at 1:250 dilution. Samples were then washed in PBS containing 0.5% Triton X-100 three

times and incubated in PBS containing 0.5% Triton X-100, 10% normal goat serum and a secondary antibody at 4°C for 24 hours. Secondary antibodies included: goat anti-rabbit 647 (Molecular Probes), goat anti-rat-647 and goat anti-mouse-488 at 1:250 dilution. Finally, brain samples were directly cleared and mounted in FocusClear™ (CelExplorer) or RapiClear 1.47 (SunJin Lab) between two coverslips separated by a 200-μm spacer ring. All samples were imaged under a LSM 880 confocal microscope with a 20x objective lens.

For anti-nc82 immunostaining, fixing was modified as follows: Samples were fixed in two stages: 1) in 4% paraformaldehyde, and 2) in 4% paraformaldehyde with 0.25% triton X-100. For each stage, samples were kept on ice in a foam box and microwaved three times for 60 seconds, briefly opening the microwave between each 60 second period.

For gut samples, fixing and washing were modified as follows: samples were fixed in 4% paraformaldehyde at 4°C for 24 hours without microwave irradiation and washed in PBS containing 0.5% Triton X-100 for 2–4 hours.

Dh31 antibody production

The rabbit polyclonal anti-Dh31 antibody was custom made by Proteintech Group, Inc (Rosemont, USA). As described previously[63], a full-length amidated Dh31 peptide (TVDFGLARGYSGTQEAKHRMGLAAANFAGGP-NH2) was synthesized and used for immunization.

Ex-vivo calcium imaging of gut endocrine cells

(1) Sample preparation and perfusion system—Male flies 6 to 8 days old were starved 24 hrs prior to dissection. Each fly gut was dissected in sugar-free adult-hemolymph like (AHL) solution[64]. The gut was opened gently with sharp forceps and then mounted on a coverslip with an EM hexagon grid (T200H-Ni, Electron Microscopy Science). To affix the grid to the coverslip, the edge of the grid was coated with vacuum grease (High-Vacuum Grease, Dow Corning). The coverslip was then flipped and sealed onto the inner side of the top of a perfusion chamber (PH1/P1 platform, JG-23 LP insert, Warner Instruments) with vacuum grease. Nutrients (Supplementary Tables 1 and 4) were dissolved in AHL at the indicated concentrations. Nutrient delivery was controlled by a perfusion system (VC-8M, Warner Instruments) driven by a peristaltic pump (ISM829, Ismatec) at the rate of 100 μL/s. The timing of solenoid valve opening was controlled by a Master-8 programmable pulse-generator (AMPI). Another peristaltic pump operating at the same rate was used to remove the waste.

(2) Image acquisition and data analysis—Images were acquired with a sCMOS camera (ORCA 4.2, HCImageLive v4.4.5.0, Hamamatsu) at a resolution of 1024 × 1024 pixels, frame rate of 0.25 Hz and exposure time of 100 ms. After image acquisition, a series of analyses were performed, including motion correction and automatic ROI identification. For motion correction, NoRMCorre[65] was used, in which the correction templates were updated every 25 frames, with a patch size of 20 pixels and an overlap of 10 pixels. For ROI identification, the maximum projection image of the video was processed by a 10×10 Gaussian filter, and the resulting image was subsequently imported into SARFIA[66] to

generate a list of ROIs. If the total number of pixels (i.e. <10) in an ROI was significantly fewer than typical cells, it was eliminated from further analysis. ROIs outside of the sample and those that failed the motion correction were also excluded from further analysis. The average pixel values were then calculated within each ROI. For each experiment, specific nutrients were delivered to the gut preparation, including 85 mM KCl at the end. If an ROI exhibited response to KCl, the corresponding cell was considered as healthy. If ΔF/F of an ROI peaks above its pre-stimulation baseline (F) more than 3.5 standard deviations of the baseline, the corresponding cell was considered to be responsive to the stimulation.

Collection of hemolymph and western blot

QIAprep 2.0 Spin Columns (QIAGEN) were used to collect fly hemolymph. Columns were first washed twice with 200 μl ddH_2O and placed in a clean 1.5 ml Eppendorf tube. 60 flies starved for 24 hrs and then fed for 2 hrs with either an amino acid mixture (200 mM), sucrose (50 mM) or a sucrose/capsaicin mixture (50 mM sucrose and 50 μM capsaicin) were placed in the column and covered with glass beads (VWR International, LLC, catalog # 26396-506) to fill the column. Tubes were centrifuged at 13,000 rpm for 20 min at 4°C and hemolymph was collected and stored at −80°C[67].

For western blots, gel electrophoresis was performed with 4 μl of the hemolymph sample. Proteins from the gel were transferred to an 0.1-μm nitrocellulose membrane (GE Healthcare Life science). After transfer, membranes were directly stained for total protein using the LI-COR REVERT™ Kit and scanned by the Odyssey® imaging system (LI-COR) at 700 nm. Membranes were boiled in PBS for 3 min and fixed in 4% paraformaldehyde at room temperature for 20 min. Membranes were then washed in PBS for 5 min and incubated in a blocking buffer (LI-COR) at room temperature for 1 hr before being incubated with the rabbit anti-Dh31 polyclonal antibody at 4°C overnight. Membranes were washed three times for five minutes with TBS containing 0.1% Triton X-100 and incubated with a 1:10000 goat anti-rabbit secondary antibody coupled to horseradish peroxidase at room temperature for 1 hr. Finally, blots were developed with the Supersignal West Femto Maximum sensitivity substrate (Thermo Fisher). The Dh31 level was normalized to total protein for quantification.

Quantitative RT-PCR

Naïve males were collected at eclosion and raised in same sex groups of 10 per vial and aged 7 days. mRNA was extracted from 6 sample sets of 5 flies each for each genotype using the QIAGEN RNeasy Mini and QIAGEN QIAshredder kits. A hand-held pestle drill was used during extraction. RNA yield was determined using a ThermoFisher Scientific NanoDrop spectrophotometer and cDNA was prepared using Invitrogen SuperScript VILO MasterMix. RT-qPCR was performed on the Bio- Rad CFX machine using iQ SYBR Green Supermix from Bio-Rad and the following primer sets: Dh31R (forward primer - CCTCCAGTACATCCTTACG, reverse primer - ATTTGGGCAATCACCTCG); and rp49 (forward primer - AGGGTATCGACAACAGAGTG, reverse primer - CACCAGGAA CTTCTTGAATC). rp49 served as a reference gene to which *Dh31R* was normalized. RT-qPCR was performed with each primer pair in three technical replicates for each cDNA sample. CT values were recorded with Bio-Rad CFX Manager software to determine relative transcript levels.

Three-photon microscopy

A three-photon microscope was custom built with a MOM scope (Sutter), a pair of 3 mm galvanometric mirrors (6210H, Cambridge Technologies), a 50 mm scan lens (SL50-3P, Thorlabs), a 200 mm tube lens (Nikon), a dichroic beamsplitter (T735LPXRXT-25 × 36, Chroma), and a high-NA objective (Olympus XLPLN25XWMP2; 25x 1.05-NA). The microscope was controlled by ScanImage 2018b (Vidrio) running on MATLAB 2019a (MathWorks). Excitation laser light at 1,320 nm was provided by an optical parametric amplifier (Opera-F, Coherent) pumped with a 1,035 nm ultrashort laser (280 fs, 1 MHz, 40 W, Monaco, Coherent). Pulse width of the excitation laser before reaching the sample was compressed down to 40 fs by a pair of prisms (10SF10, Newport Corporation). Average laser power was controlled by a half-wave plate (AHWP05M-1600, Thorlabs) and a polarizing beamsplitter (PBS054, Thorlabs). Laser power at 3–4 mW, after the microscope objective, was used to image brain neurons. Fluorescence light and the third harmonic generation (THG) signal were separated by a 488-nm dichroic beamsplitter (Di02-R488-25 × 36, Semrock) and each path was filtered by a band-pass filter. Fluorescence: a 525 ± 35 nm (ET525/70m-2p, Chroma); THG: a 445 ± 10 nm (FF01-445/20, Semrock). Fluorescence and THG signals were detected by two different GaAsP PMTs (Hamamatsu), H11706-40 and H10770B-40, respectively. PMT current was converted to voltage by a transimpedance amplifier (150 kΩ, 1 MHz low-pass, XPG-ADC-PREAMP, Sigmann Elektronik), and digitized by a data acquisition module (PXIe-1073NI-5732, PXIe-6341, PXIe-7961, National Instruments). All images were acquired at a resolution of 512 × 512 pixels (0.205 × 0.205 μm/pixel).

Transcuticle imaging of intact fly

Under CO_2 anesthesia, individual male flies were mounted onto the edge of a coverglass at the posterior side of their heads using glue (Bondic). UV light was then used to cure the glue for 5 seconds. For imaging, the coverglass was mounted on a custom fly holder and deuterated water was used as an immersion medium to minimize laser absorption. For Dh31 peptide injection, a sharp electrode was first filled with 10 μM Dh31 synthetic peptide. Dh31 peptide, [Acetyl-TVDFGLARGYSGTQEAKHRMGLAAANFAGGP], [99.32%] (Celtek Bioscience) was dissolved in sugar-free AHL saline[64]. To inject the Dh31 peptide solution, the electrode tip was broken and inserted into the dorsal vessel[68] of the tethered fly. The solution was then injected using a syringe. For optogenetic stimulation of gut cells, a piece of black aluminum foil was used to shield the fly head from light exposure. Images were acquired at 0.5 frame/s and interleaved by 800-ms optogenetic stimulation (660 nm). For the effect of cardiac arrest on the response of corazonin neurons to optogenetically activated gut Dh31 cells, the fly prep was placed in a 2.1 mL enclosure and flooded with CO_2 for 10 s at the rate of 1,000 mL/min.

Heartbeat visualization

Fluorescence microscopy was used to monitor heartbeat frequency of male flies. For visualization, the cardiomyocyte specific enhancer R94C02 was used to drive the expression of tdTomato[69]. After being deprived of food for 24 hrs, 7-day old males were anesthetized and glued to a coverglass at the dorsal side. Individual flies were then placed in a 2.1 mL

enclosure. The heart tube was imaged with a water immersion objective (Olympus LUMFL N; 60x 1.10-NA) at the second abdominal segment. Flies were given 10 min to recover from CO_2 anesthesia before image acquisition (CoolSNAP HQ2 CCD camera and μManager 1.4, 30 frame/s, 174 × 130 pixels). Baseline heart activity was recorded for 5 minutes before the enclosure was flooded with CO_2 for 10 s at a rate of 1,000 mL/min. The heartbeat frequency was derived from the images and presented in 30-s intervals.

CaLexA measurement

Dissected brains of 5-day old male flies were immunostained with an anti-Crz antibody following the protocol outlined in the Immunofluorescence section. Sample preparation and imaging were done in parallel to evaluate the impact of food nutrient composition on the intracellular Ca^{2+} level of Crz^{+} neurons. For image acquisition, laser power and detector gain were held constant across samples. Confocal images were processed in imageJ (NIH). First, a plane of maximum anti-Crz fluorescence was selected to analyze individual cells. Then a region of interest (ROI) outlining the cell body was drawn. The average CaLexA signal from each ROI was then registered after subtracting the background signal. The background signal was measured by selecting a region that has no fluorescence near the cells of interest.

Extended Data

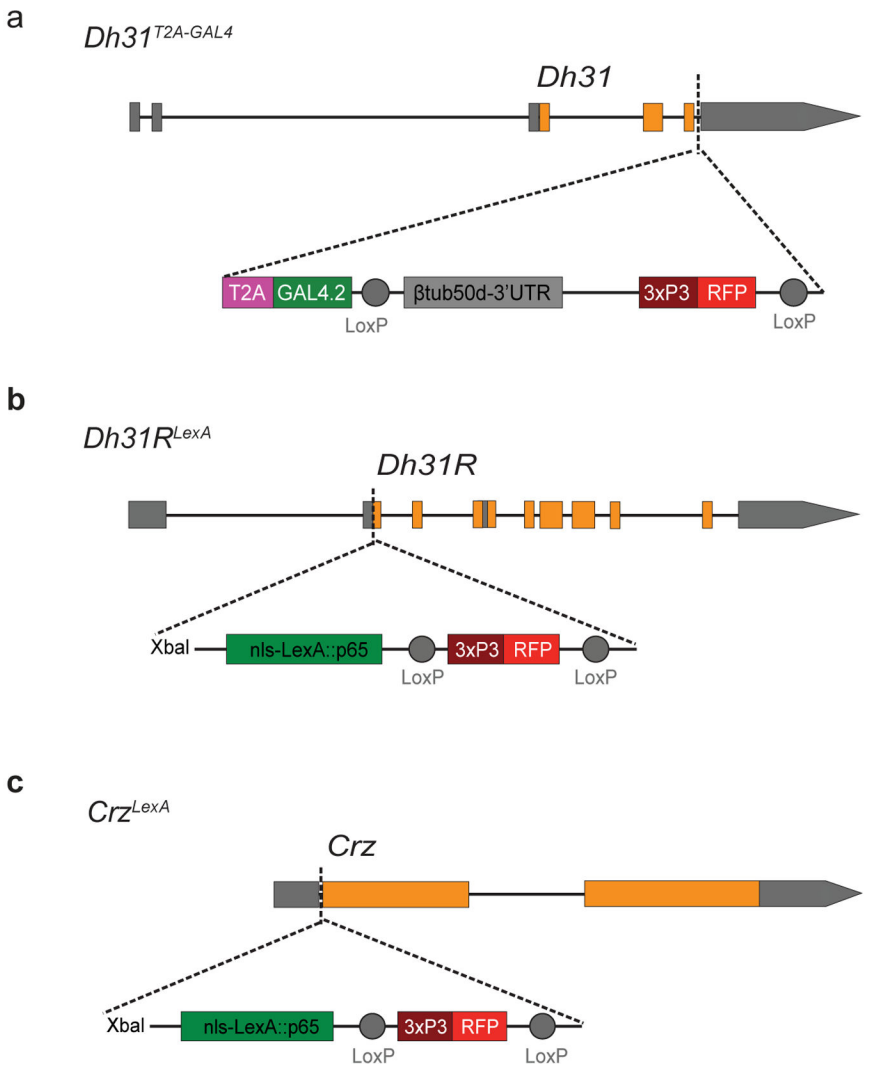

Extended Data Figure 1. Schematic illustration of gene structures and knock-in constructs

(a) A *T2A-GAL4.2* cassette was inserted at the C-terminus of *Dh31* by Cas9-mediated knock-in strategy. 3XP3-RFP was used as a positive selection marker.

(b) An *nls-LexA::p65* cassette was inserted after the start codon of *Dh31R* by Cas9-mediated knock-in strategy.

(c) An *nls-LexA::p65* cassette was inserted after the start codon of *Crz* by Cas9-mediated knock-in strategy.

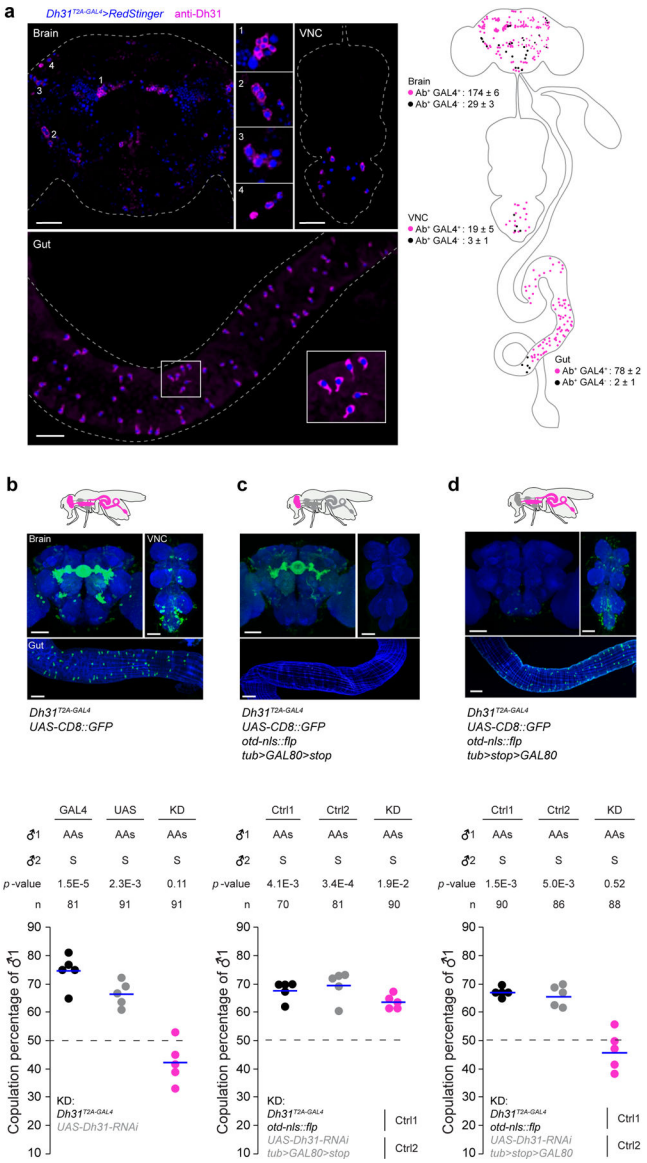

Extended Data Figure 2. Dh31 expression outside the brain is required for the effect of ingested amino acids on courtship

(a) Validation of the *Dh31*$^{T2A\text{-}GAL4}$ driver line by a Dh31 antiserum. Representative confocal images show the expression pattern of *Dh31*$^{T2A\text{-}GAL4}$ (Blue) and Dh31 (magenta) in the brain, ventral nerve cord (VNC) and midgut of male flies carrying *Dh31*$^{T2A\text{-}GAL4}$ and UAS-*Redstinger*. Schematic indicates the organization of Dh31 cells in the brain, VNC, and GI tract, drawn from the confocal stacks of the sample shown in the left panel. Magenta dots show cell positive for Dh31 antibody and Redstinger; black dots show cells positive for Dh31 antibody and negative for Redstinger. The average number (± SEM) of cells in each region is from 5 different male flies. Scale bar, 50 μm.

(b-d) The courtship effect of region-specific *Dh31* knockdown. *Dh31* knockdown in all *Dh31*$^{T2A\text{-}GAL4}$ cells (b); *Dh31* knockdown in brain *Dh31*$^{T2A\text{-}GAL4}$ cells (c); *Dh31* knockdown in *Dh31*$^{T2A\text{-}GAL4}$ cells outside the brain (d). The total number of matches (n) is shown, with 5 experiments per condition and 12–24 successful matches per experiment.

p-value was determined by Chi-square test to indicate whether males of a given genetic manipulation respond to amino acids. Blue bar indicates average copulation percentage, and the dashed line indicates chance level.

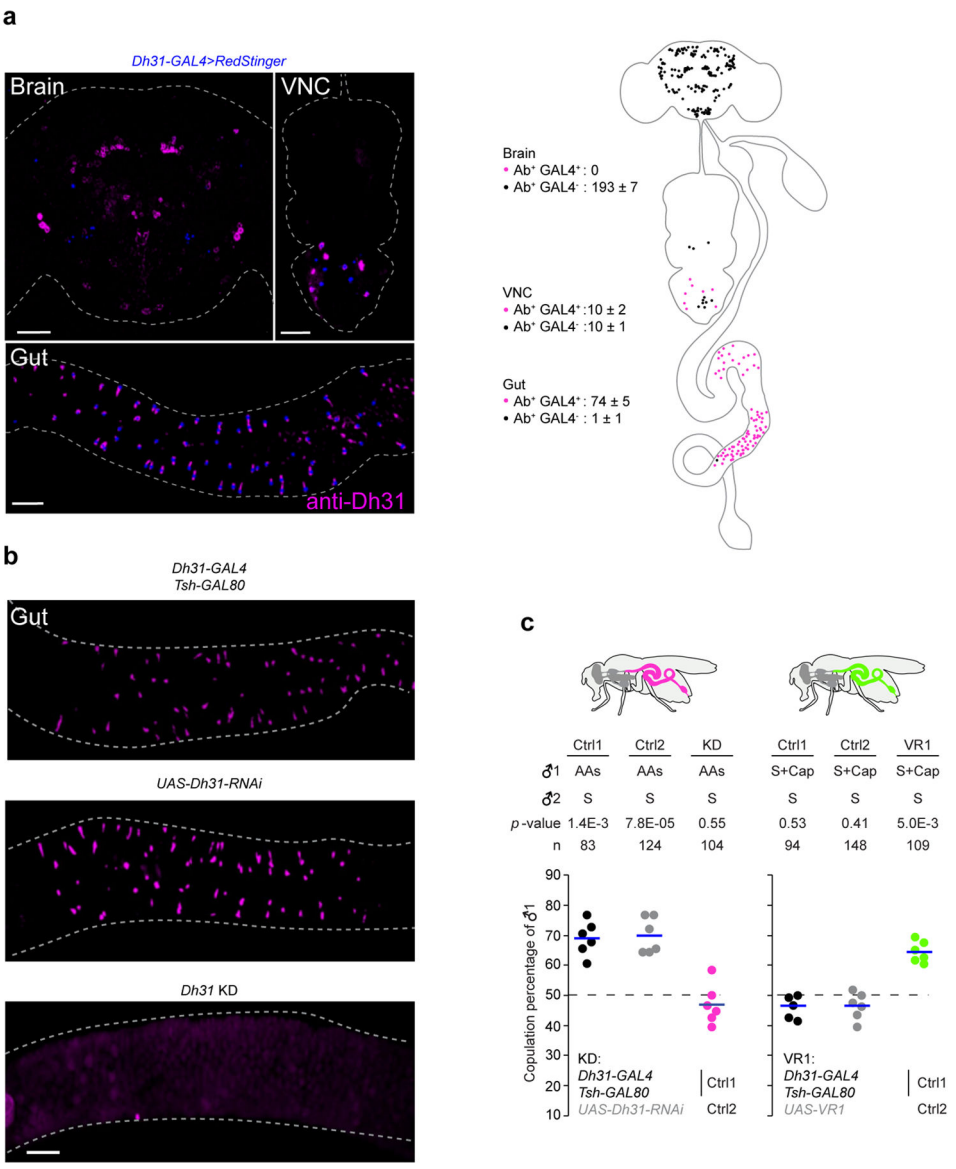

Extended Data Figure 3. Dh31 expression in enteroendocrine cells is required for the effect of ingested amino acids

(a) Expression of Redstinger (blue) and Dh31 (anti-Dh31, magenta) in the brain, VNC and midgut of a male containing *Dh31-GAL4* and *UAS-Redstinger*. Scale bar, 50 μm. Schematic indicates the organization of cell clusters in the brain, VNC and GI tract, drawn from the confocal stacks of the sample shown in the left panel. Magenta dots: Dh31 antibody^{+} and GAL4^{+} cells; black dots: Dh31 antibody^{+} and GAL4^{-} cells. The average number (± SEM) of cells in each region is from 5 different male flies.

(b) Validation of *Dh31* knockdown. Knockdown of *Dh31* in the gut is achieved by using *Dh31-GAL4* and *Tsh-GAL80* to drive *UAS-Dh31-RNAi*. Immunostaining with an antiserum to Dh31 (magenta) shows that knockdown is effective in the gut. Scale bar, 50 μm.
(c) The courtship effect of gut-specific *Dh31* knockdown (left) or chemo-activation of gut Dh31$^+$ cells (right). Chemo-activation is achieved by using *Dh31-GAL4* and *Tsh-GAL80* to drive *UAS-VR1*. The total number of matches (n) is shown, with 5–6 experiments per condition and 12–28 successful matches per experiment. *p*-value was determined by Chi-square test to indicate whether males of a given genetic manipulation respond to amino acids (left) or capsaicin (right). Blue bar indicates average copulation percentage, and the dashed line indicates chance level.

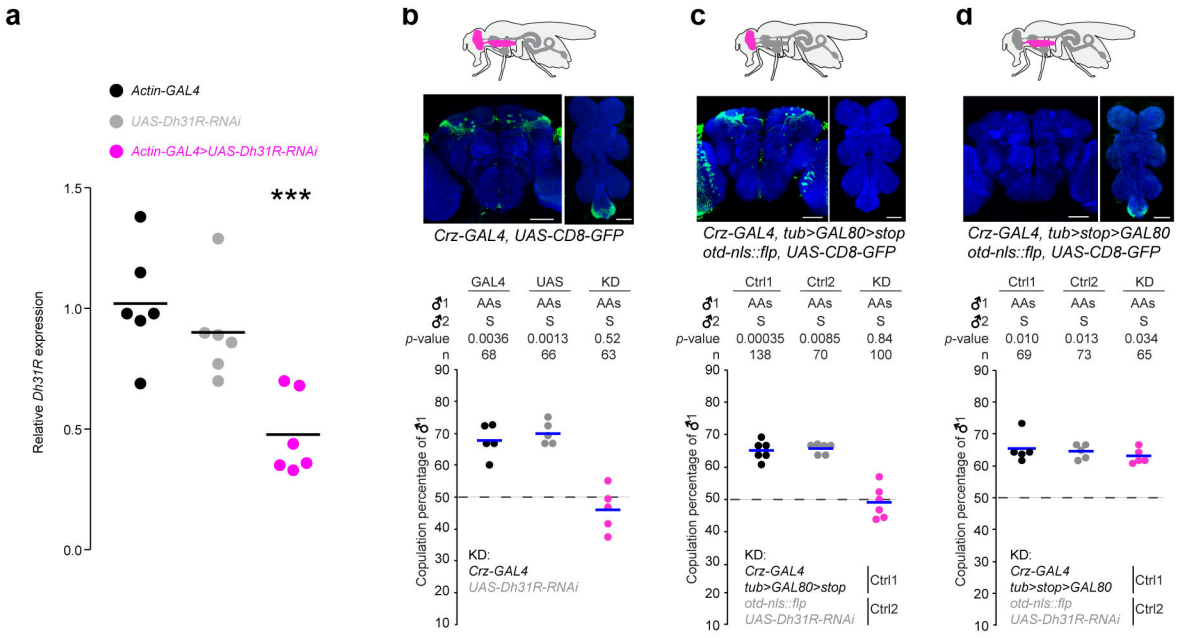

Extended Data Figure 4. Expression of Dh31R in brain Crz$^+$ neurons is required for the aphrodisiac effect of amino acids

(a) Validation of *Dh31R* knockdown. qRT-PCR results show that *Dh31R* expression level is reduced in flies having the *Actin-GAL4* and *UAS-Dh31R-RNAi* transgenes. RNA was extracted from 5 male flies per experiment, with 6 experiments for each genotype.
(b-d) Schematic indicates genetic strategies to perturb Crz$^+$ neurons in the brain and VNC (b), only in the brain (c), and only in the VNC (d). Representative confocal images show the different intersections between *Crz-GAL4* and *otd-nls::flp* (corresponding genotypes are shown below the images). Samples were immuostained with anti-GFP (green), nc82 (blue). Scale bar, 50 μm. The courtship effect of *Dh31R* knockdown in both brain and VNC, in brain only or in VNC only. The total number of matches (n) is shown, with 5–6 experiments per condition and 8–26 successful matches per experiment. *p*-value was determined by Chi-square test to indicate whether males of a given genetic manipulation respond to amino acids. Blue bar indicates average copulation percentage, and the dashed line indicates chance level.

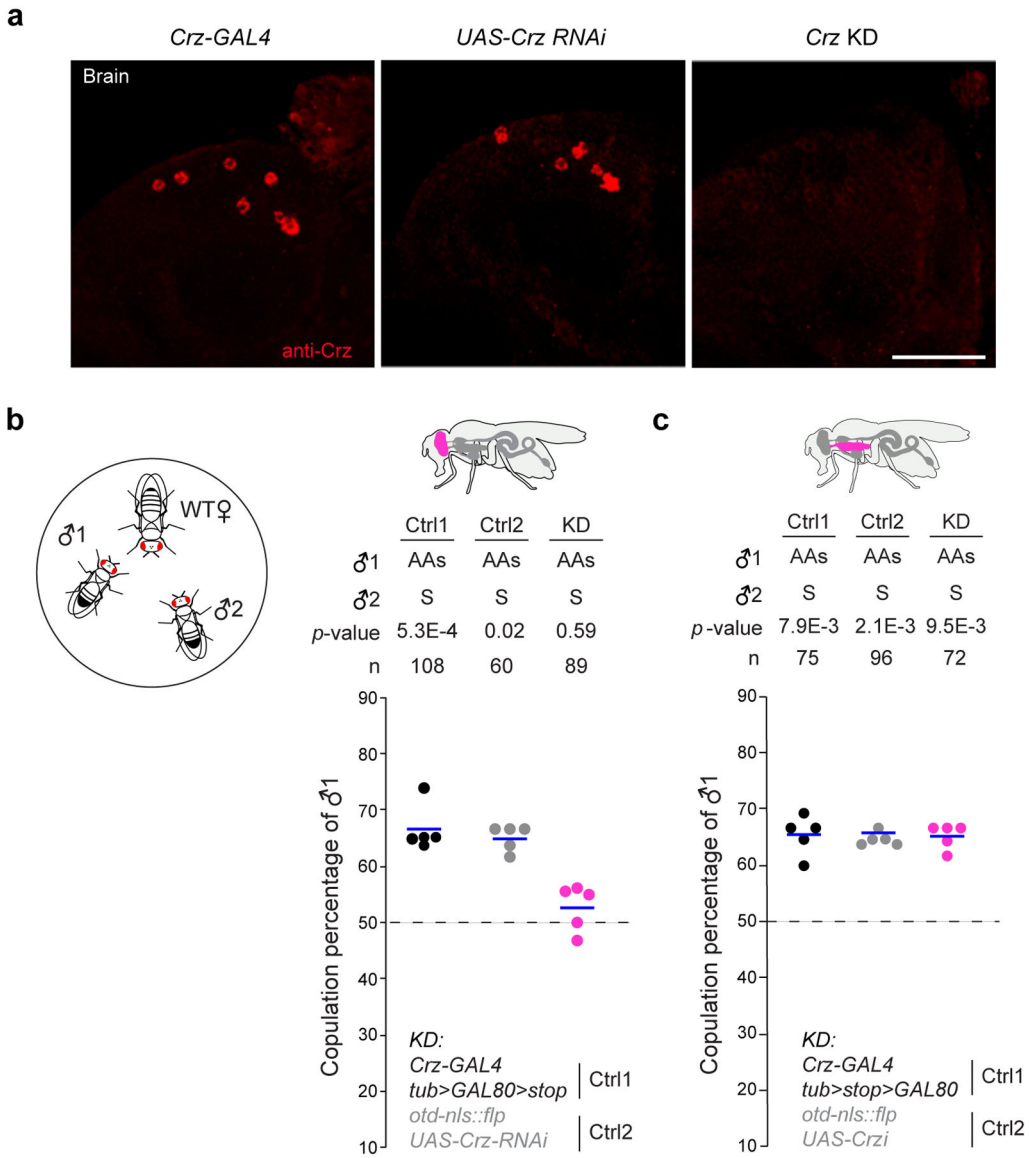

Extended Data Figure 5. Expression of Crz in brain Crz$^+$ neurons is required for the aphrodisiac effect of amino acids

(a) Validation of *Crz* knockdown. Immunostaining of anti-Crz (red) showed Crz is undetectable in brain Crz$^+$ neurons in *Crz-Gal4*, *UAS-Crz-RNAi* flies. Scale bar, 50 μm. (b and c) The courtship effect of *Crz* knockdown in brain Crz$^+$ neurons (b) or in VNC Crz$^+$ neurons (c). The total number of matches (n) is shown, with 5 experiments per condition and 11–23 successful matches per experiment. *p*-value was determined by Chi-square test to indicate whether males of a given genetic manipulation respond to amino acids. Blue bar indicates average copulation percentage, and the dashed line indicates chance level.

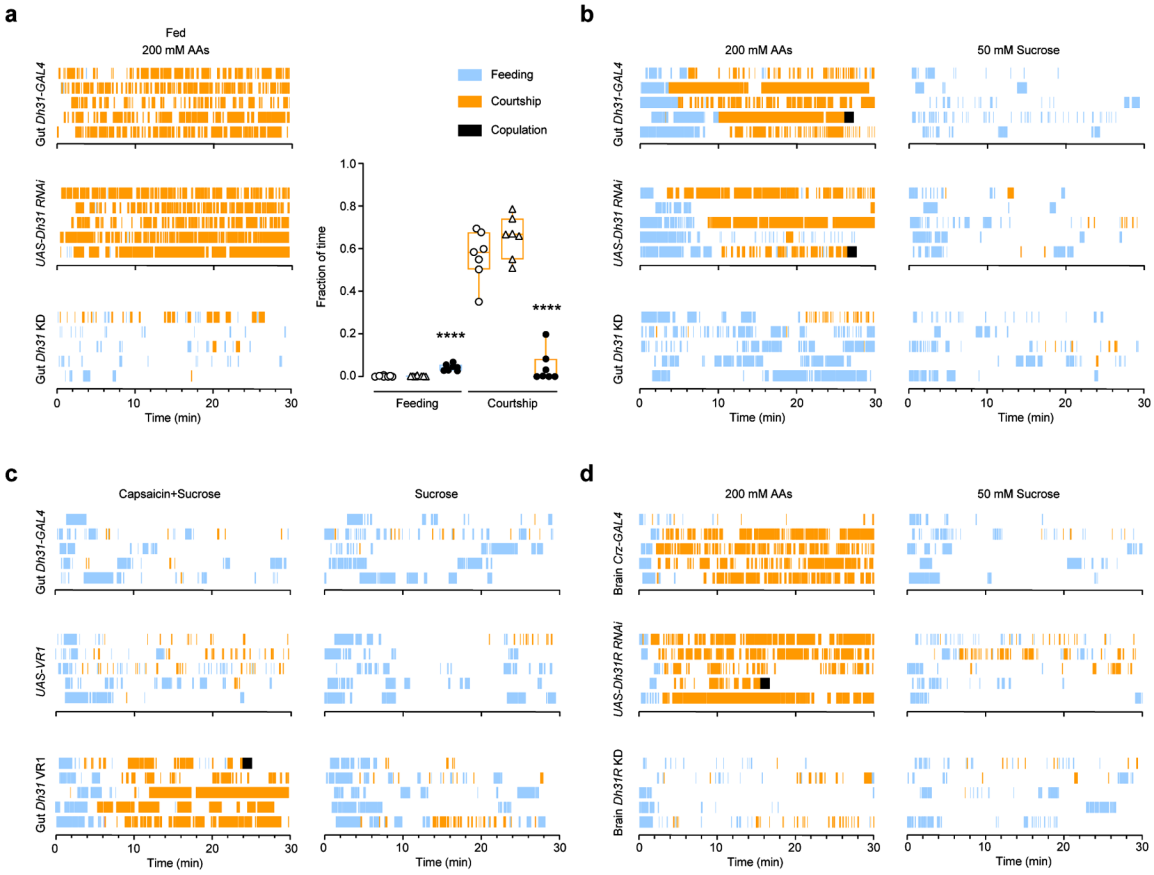

Extended Data Figure 6. Dh31 in the gut and Dh31R in brain Crz$^+$ neurons are required for males to transition from feeding to courtship

(a, b) The effect of gut-specific *Dh31* knockdown on feeding and courtship in fed (a) or starved (b) flies. The knockdown increased feeding duration and eliminated courtship when food contained amino acids, but had no effect when food contained only sucrose. GAL4: *Dh31-GAL4*, *Tsh-GAL80*. UAS: *UAS-Dh31-RNAi*. Gut *Dh31* KD flies had all three transgenes. The fraction of time individual males spent on feeding and courtship in (a). n = 7 for each condition. ****, $p < 0.0001$, ANOVA followed by Tukey's test.

(c) Chemo-activation of gut *Dh31-GAL4* cells. The ingestion of capsaicin-containing food induced courtship but food containing only sucrose had no effect. GAL4: *Dh31-GAL4*, *Tsh-GAL80*. UAS: *UAS-VR1*. Gut *Dh31* VR1 flies had all three transgenes.

(d) *Dh31R* knockdown in brain Crz$^+$ neurons eliminated the effect of amino acids on courtship, but not feeding. GAL4: *Crz-GAL4*, *tub>GAL80>stop*. UAS: *otd-nls::flp*, *UAS-Dh31R-RNAi*. Brain *Dh31R* KD flies had all four transgenes.

The Raster Plots show the second-by-second behaviors of 5 representative males. Behaviors: feeding (blue), courtship (orange) and copulation (black).

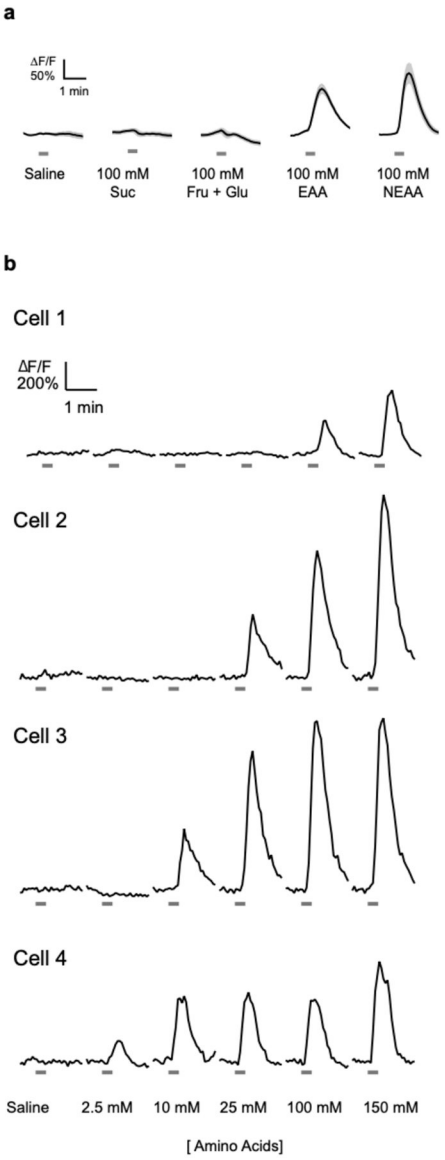

Extended Data Figure 7. Dh31 enteroendocrine cells respond to amino acids

(a) Response of Dh31^{+} cells to different nutrients at the indicated concentrations. Suc: sucrose, Fru + Glu: mixture of fructose and glucose, EAA: essential amino acids, NEAA: nonessential amino acids. The average calcium response (ΔF/F) is shown in black with SEM as gray shaded areas (n=6).

(b) The response of individual Dh31^{+} cells to amino acids at different concentrations. Gray lines below the traces indicate the stimulation period of amino acids or saline control.

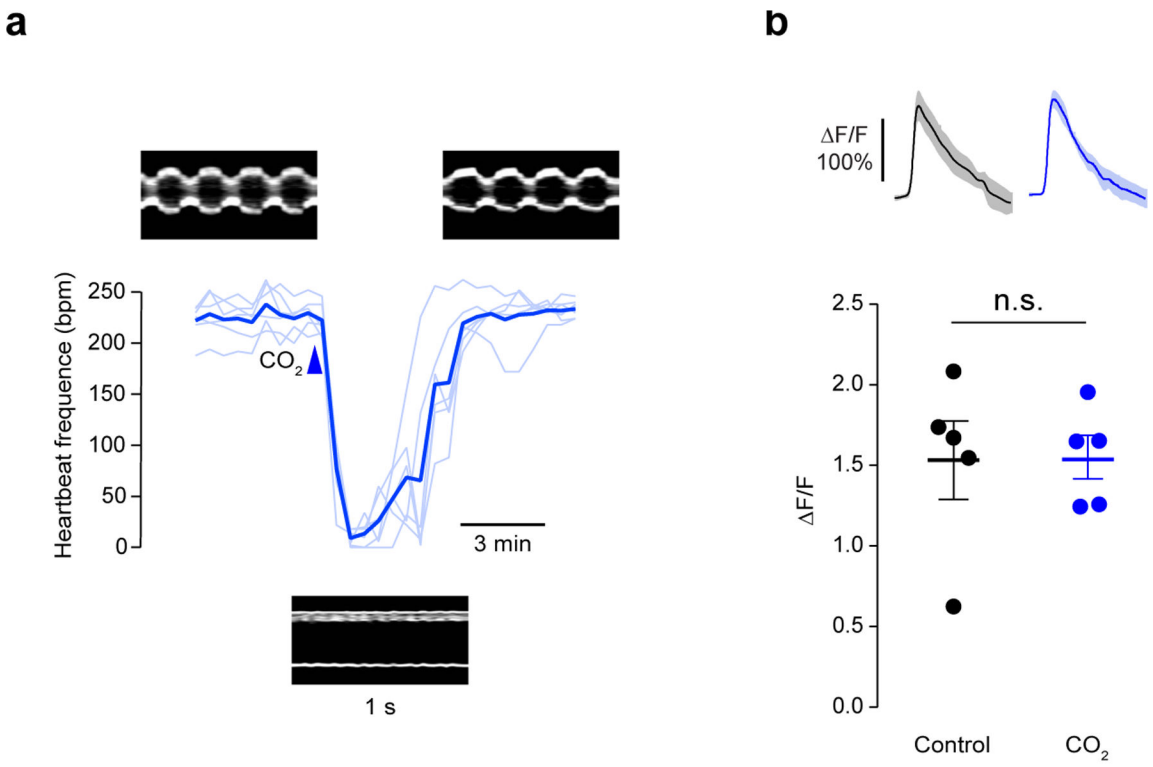

Extended Data Figure 8. Effect of CO_2 exposure on heartbeat and the response of brain Crz^+ neurons to the activation of gut $Dh31^+$ cells

(a) Images show the changing diameter of the heart-tube before, during and after CO_2 exposure. Heartbeat frequency was extracted from the changing diameter in male flies expressing tdTomato in cardiomyocytes. The light and dark blue lines show the heartbeat frequency of individual flies and the average, respectively (n=6).

(b) The effect of CO_2-exposure on the peak ΔF/F of Crz^+ neurons in response to optogenetic activation of $Dh31^+$ enteroendocrine cells. Stimulation intensity: 1.75 mW/mm^2. n.s., not significant, t-test (n = 5).

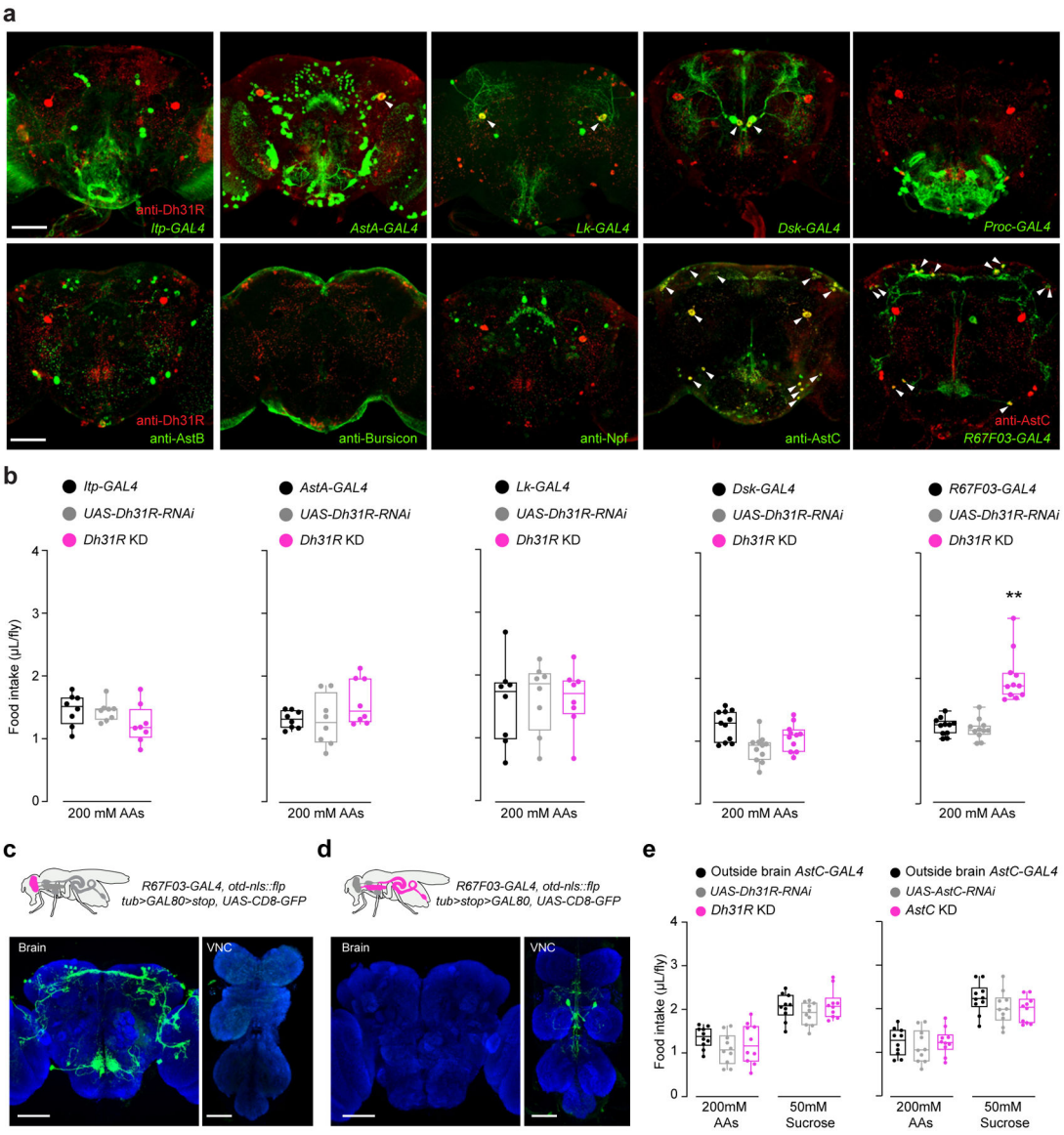

Extended Data Figure 9. Identification of brain Dh31R^{+} neurons that regulate the intake of protein-containing food

(a) Expression pattern of neuropeptides, neuropeptidergic driver lines and Dh31R in the brain. Top row: arrowheads indicate neurons that co-express Dh31R with *AstA-GAL4*, *Lk-GAL4*, or *Dsk-GAL4*. Bottom row: arrowheads indicate neurons that co-express AstC with Dh31R or *R67F03-GAL4*. Scale bar, 50 µm.

(b) Food intake of flies with *Dh31R* knockdown in different neurons. Gal4 lines (*Itp*, *AstA*, *LK*, *R67F03*) were crossed to *UAS-Dh31R-RNAi* and tested for amino acid food consumption. Male flies with *Dh31R* knockdown in *R67F03-GAL4* cells consumed more amino acids than controls.

(c and d) Genetic strategies to label *R67F03-GAL4* neurons in the brain (c) and outside the brain (d). Representative confocal images show the different intersections between *R67F03-GAL4* and *otd-nls::flp* (corresponding genotypes are shown). Samples were immunostained with anti-GFP (green), nc82 (blue). Scale bar, 50 µm.

(e) Knockdown of *Dh31R* (left panel) or *AstC* in *R67F03-GAL4* cells outside the brain. Knockdown male flies consumed the same amount of amino acids and sucrose food compared with control flies. GAL4*: R67F03-GAL4*, *otd-nls*::*flp*; UAS: *UAS-Dh31R-RNAi, tub>stop>GAL80*; *Dh31R* KD flies have all four transgenes (left panel). GAL4*: R67F03-GAL4*, *otd-nls*::*flp*; UAS: *UAS-AstC-RNAi, tub>stop>GAL80*; *AstC* KD flies have all four transgenes (right panel). 8–11 experiments for each condition/genotype. **, $p < 0.01$, ANOVA followed by Tukey's test.

Supplementary Material

Refer to Web version on PubMed Central for supplementary material.

ACKNOWLEDGMENT

We thank David Kleinfeld, Chih-Ying Su and Kenta Asahina for comments on the manuscript. We thank Yishi Jin for sharing the spectrophotometer. We thank David Kleinfeld and Chris Xu for continuous advice on three-photon microscopy. We thank the following individuals for reagents: Jan Veenstra (Dh31, AstB and AstC antiserum), Benjamin White (Bursicon antiserum), Fumika Hamada (Dh31R antiserum), and Rolf Bodmer (R94C02::tdTomato transgenic line). We also thank members of the Wang lab and Su lab for stimulating discussions. Confocal imaging was supported by NINDS P30 NS047101 (UC San Diego Neuroscience MicroscopyImaging Core). I.H. and M.R. acknowledge funding from the National Science Foundation (1429810). This work was supported by NIH grants to J.W.W. (R01DK127516, R01DK092640, R01DC009597) and to H.-H.L. (K99DC016338).

REFERENCES

1. Tinbergen N The Study of Instinct. (Clarendon Press, 1951).
2. McFarland DJ Decision making in animals. Nature 269, 15–21 (1977).
3. Stearns SC The Evolution of Life Histories. (OUP Oxford, 1992).
4. Roff D Evolution Of Life Histories: Theory and Analysis. (Springer US, 1993).
5. Sutton AK & Krashes MJ Integrating Hunger with Rival Motivations. Trends Endocrinol. Metab 31, 495–507 (2020). [PubMed: 32387196]
6. Morton GJ, Meek TH & Schwartz MW Neurobiology of food intake in health and disease. Nat. Rev. Neurosci 15, 367–378 (2014). [PubMed: 24840801]
7. Inagaki HK et al. Visualizing neuromodulation in vivo: TANGO-mapping of dopamine signaling reveals appetite control of sugar sensing. Cell 148, 583–595 (2012). [PubMed: 22304923]
8. Marella S, Mann K & Scott K Dopaminergic modulation of sucrose acceptance behavior in *Drosophila*. Neuron 73, 941–950 (2012). [PubMed: 22405204]
9. Hadjieconomou D et al. Enteric neurons increase maternal food intake during reproduction. Nature 587, 455–459 (2020). [PubMed: 33116314]
10. Karigo T et al. Distinct hypothalamic control of same- and opposite-sex mounting behaviour in mice. Nature 589, 258–263 (2021). [PubMed: 33268894]
11. Bayless DW et al. Limbic neurons shape sex recognition and social behavior in sexually naive males. Cell 176, 1190–1205 (2019). [PubMed: 30712868]
12. Yang CF et al. Sexually dimorphic neurons in the ventromedial hypothalamus govern mating in both sexes and aggression in males. Cell 153, 896–909 (2013). [PubMed: 23663785]
13. Dickson BJ Wired for Sex: The neurobiology of *Drosophila* mating decisions. Science 322, 904–909 (2008). [PubMed: 18988843]
14. Yamamoto D, Sato K & Koganezawa M Neuroethology of male courtship in *Drosophila*: from the gene to behavior. J. Comp. Physiol. A. Neuroethol. Sens. Neural. Behav. Physiol 200, 251–264 (2014). [PubMed: 24567257]
15. Zhang SX, Rogulja D & Crickmore MA Dopaminergic circuitry underlying mating drive. Neuron 91, 168–181 (2016). [PubMed: 27292538]

16. Fricke C, Bretman A & Chapman T Adult male nutrition and reproductive success in *Drosophila melanogaster*. Evolution 62, 3170–3177 (2008). [PubMed: 18786187]
17. Piper MDW et al. A holidic medium for *Drosophila melanogaster*. Nat. Methods 11, 100–105 (2014). [PubMed: 24240321]
18. Lin H-H et al. Hormonal modulation of pheromone detection enhances male courtship success. Neuron 90, 1272–1285 (2016). [PubMed: 27263969]
19. Schneider JE, Wise JD, Benton NA, Brozek JM & Keen-Rhinehart E When do we eat? Ingestive behavior, survival, and reproductive success. Horm. Behav 64, 702–728 (2013). [PubMed: 23911282]
20. Guo X et al. The Cellular diversity and transcription factor code of *Drosophila* enteroendocrine cells. Cell Rep. 29, 4172–4185 (2019). [PubMed: 31851941]
21. Hung R-J et al. A cell atlas of the adult *Drosophila* midgut. Proc. Natl. Acad. Sci. U. S. A 117, 1514–1523 (2020). [PubMed: 31915294]
22. Veenstra JA & Ida T More *Drosophila* enteroendocrine peptides: Orcokinin B and the CCHamides 1 and 2. Cell Tissue Res. 357, 607–621 (2014). [PubMed: 24850274]
23. Park J-H et al. A subset of enteroendocrine cells is activated by amino acids in the *Drosophila* midgut. FEBS Lett. 590, 493–500 (2016). [PubMed: 26801353]
24. Bellen HJ et al. The BDGP Gene disruption project. Genetics 167, 761–781 (2004). [PubMed: 15238527]
25. Asahina K et al. Tachykinin-expressing neurons control male-specific aggressive arousal in *Drosophila*. Cell 156, 221–235 (2014). [PubMed: 24439378]
26. Hergarden AC, Tayler TD & Anderson DJ Allatostatin-A neurons inhibit feeding behavior in adult *Drosophila*. Proc. Natl. Acad. Sci 109, 3967–3972 (2012). [PubMed: 22345563]
27. Tayler TD, Pacheco DA, Hergarden AC, Murthy M & Anderson DJ A neuropeptide circuit that coordinates sperm transfer and copulation duration in *Drosophila*. Proc. Natl. Acad. Sci 109, 20697–20702 (2012). [PubMed: 23197833]
28. Clyne JD & Miesenböck G Sex-Specific Control and Tuning of the Pattern Generator for Courtship Song in *Drosophila*. Cell 133, 354–363 (2008). [PubMed: 18423205]
29. Marella S et al. Imaging taste responses in the fly brain reveals a functional map of taste category and behavior. Neuron 49, 285–295 (2006). [PubMed: 16423701]
30. Jordt S-E & Julius D Molecular basis for species-specific sensitivity to 'hot' chili peppers. Cell 108, 421–430 (2002). [PubMed: 11853675]
31. Johnson EC et al. A novel diuretic hormone receptor in *Drosophila*: evidence for conservation of CGRP signaling. J. Exp. Biol 208, 1239–1246 (2005). [PubMed: 15781884]
32. Dana H et al. High-performance calcium sensors for imaging activity in neuronal populations and microcompartments. Nat. Methods 16, 649–657 (2019). [PubMed: 31209382]
33. Tao X et al. Transcutical imaging with cellular and subcellular resolution. Biomed. Opt. Express 8, 1277–1289 (2017). [PubMed: 28663828]
34. Klapoetke NC et al. Independent optical excitation of distinct neural populations. Nat. Methods 11, 338–346 (2014). [PubMed: 24509633]
35. Badre NH, Martin ME & Cooper RL The physiological and behavioral effects of carbon dioxide on *Drosophila melanogaster* larvae. Comp. Biochem. Physiol. A. Mol. Integr. Physiol 140, 363–376 (2005). [PubMed: 15792602]
36. Masuyama K, Zhang Y, Rao Y & Wang JW Mapping neural circuits with activity-dependent nuclear import of a transcription factor. J. Neurogenet 26, 89–102 (2012). [PubMed: 22236090]
37. Wu Q et al. Excreta Quantification (EX-Q) for longitudinal measurements of food intake in *Drosophila*. iScience 23, 100776 (2020). [PubMed: 31901635]
38. Al-Anzi B et al. The Leucokinin pathway andIts neurons regulate meal size in *Drosophila*. Curr. Biol 20, 969–978 (2010). [PubMed: 20493701]
39. Clark L, Zhang JR, Tobe S & Lange AB Proctolin: A possible releasing factor in the corpus cardiacum/corpus allatum of the locust. Peptides 27, 559–566 (2006). [PubMed: 16309785]

40. Down RE, Matthews HJ & Audsley N Effects of Manduca sexta allatostatin and an analog on the pea aphid Acyrthosiphon pisum (Hemiptera: Aphididae) and degradation by enzymes from the aphid gut. Peptides 31, 489–497 (2010). [PubMed: 19560498]
41. Gáliková M, Dircksen H & Nässel DR The thirsty fly: Ion transport peptide (ITP) is a novel endocrine regulator of water homeostasis in *Drosophila*. PLOS Genet. 14, e1007618 (2018). [PubMed: 30138334]
42. Min S et al. Identification of a peptidergic pathway critical to satiety responses in *Drosophila*. Curr. Biol 26, 814–820 (2016). [PubMed: 26948873]
43. Scopelliti A et al. A neuronal relay mediates a nutrient responsive gut/fat body axis regulating energy homeostasis in adult *Drosophila*. Cell Metab. 29, 269–284 (2019). [PubMed: 30344016]
44. Söderberg JAE, Carlsson MA & Nässel DR Insulin-producing cells in the *Drosophila* brain also express satiety-inducing Cholecystokinin-like peptide, *Drosulfakinin*. Front. Endocrinol 3, 109 (2012).
45. Wu Q et al. Developmental control of foraging and social behavior by the *Drosophila* neuropeptide Y-like system. Neuron 39, 147–161 (2003). [PubMed: 12848939]
46. Pfeiffer BD et al. Refinement of tools for targeted gene expression in *Drosophila*. Genetics 186, 735–755 (2010). [PubMed: 20697123]
47. Maslow AH & Press G A Theory of Human Motivation. (General Press, 2019).
48. Alhadeff AL et al. A neural circuit for the suppression of pain by a competing need state. Cell 173, 140–152 (2018). [PubMed: 29570993]
49. Partridge L, Gems D & Withers DJ Sex and Death: What Is the connection? Cell 120, 461–472 (2005). [PubMed: 15734679]
50. Hewes RS & Taghert PH Neuropeptides and neuropeptide receptors in the *Drosophila melanogaster* genome. Genome Res. 11, 1126–1142 (2001). [PubMed: 11381038]
51. Temple JL & Rissman EF Acute re-feeding reverses food restriction-induced hypothalamic-pituitary-gonadal Axis Deficits1. Biol. Reprod 63, 1721–1726 (2000). [PubMed: 11090441]
52. Zimmerman CA et al. A gut-to-brain signal of fluid osmolarity controls thirst satiation. Nature 568, 98–102 (2019). [PubMed: 30918408]
53. Augustine V, Gokce SK & Oka Y Peripheral and central nutrient sensing underlying appetite regulation. Trends Neurosci. 41, 526–539 (2018). [PubMed: 29914721]
54. Carter ME, Soden ME, Zweifel LS & Palmiter RD Genetic identification of a neural circuit that suppresses appetite. Nature 503, 111–114 (2013). [PubMed: 24121436]
55. Saper CB, Fuller PM, Pedersen NP, Lu J & Scammell TE Sleep state switching. Neuron 68, 1023–1042 (2010). [PubMed: 21172606]
56. Jourjine N, Mullaney BC, Mann K & Scott K Coupled sensing of hunger and thirst signals balances sugar and water consumption. Cell 166, 855–866 (2016). [PubMed: 27477513]
57. Oh Y et al. A glucose-sensing neuron pair regulates insulin and glucagon in *Drosophila*. Nature 574, 559–564 (2019). [PubMed: 31645735]
58. Flavell SW et al. Serotonin and the neuropeptide PDF initiate and extend opposing behavioral states in *C. elegans*. Cell 154, 1023–1035 (2013). [PubMed: 23972393]
59. Kondo S & Ueda R Highly improved gene targeting by germline-specific Cas9 expression in *Drosophila*. Genetics 195, 715–721 (2013). [PubMed: 24002648]
60. Veenstra JA, Agricola H-J & Sellami A Regulatory peptides in fruit fly midgut. Cell Tissue Res. 334, 499–516 (2008). [PubMed: 18972134]
61. Peabody NC et al. Bursicon Functions within the *Drosophila* CNS to Modulate Wing Expansion Behavior, Hormone Secretion, and Cell Death. J. Neurosci 28, 14379–14391 (2008). [PubMed: 19118171]
62. Goda T et al. Calcitonin receptors are ancient modulators for rhythms of preferential temperature in insects and body temperature in mammals. Genes Dev. 32, 140–155 (2018). [PubMed: 29440246]
63. Kunst M et al. Calcitonin gene-related peptide neurons mediate sleep-specific circadian output in *Drosophila*. Curr. Biol 24, 2652–2664 (2014). [PubMed: 25455031]

64. Wang JW, Wong AM, Flores J, Vosshall LB & Axel R Two-photon calcium imaging reveals an odor-evoked map of activity in the fly brain. Cell 112, 271–282 (2003). [PubMed: 12553914]

65. Pnevmatikakis EA & Giovannucci A NoRMCorre: An online algorithm for piecewise rigid motion correction of calcium imaging data. J. Neurosci. Methods 291, 83–94 (2017). [PubMed: 28782629]

66. Dorostkar MM, Dreosti E, Odermatt B & Lagnado L Computational processing of optical measurements of neuronal and synaptic activity in networks. J. Neurosci. Methods 188, 141–150 (2010). [PubMed: 20152860]

67. Lindsay SA, Lin SJH & Wasserman SA Short-Form Bomanins Mediate Humoral Immunity in *Drosophila*. J. Innate Immun 10, 306–314 (2018). [PubMed: 29920489]

68. Lee J, Iyengar A & Wu C-F Distinctions among electroconvulsion- and proconvulsant-induced seizure discharges and native motor patterns during flight and grooming: quantitative spike pattern analysis in *Drosophila* flight muscles. J. Neurogenet 33, 125–142 (2019). [PubMed: 30982417]

69. Klassen MP et al. Age-dependent diastolic heart failure in an in vivo *Drosophila* model. Elife 6, e20851 (2017). [PubMed: 28328397]

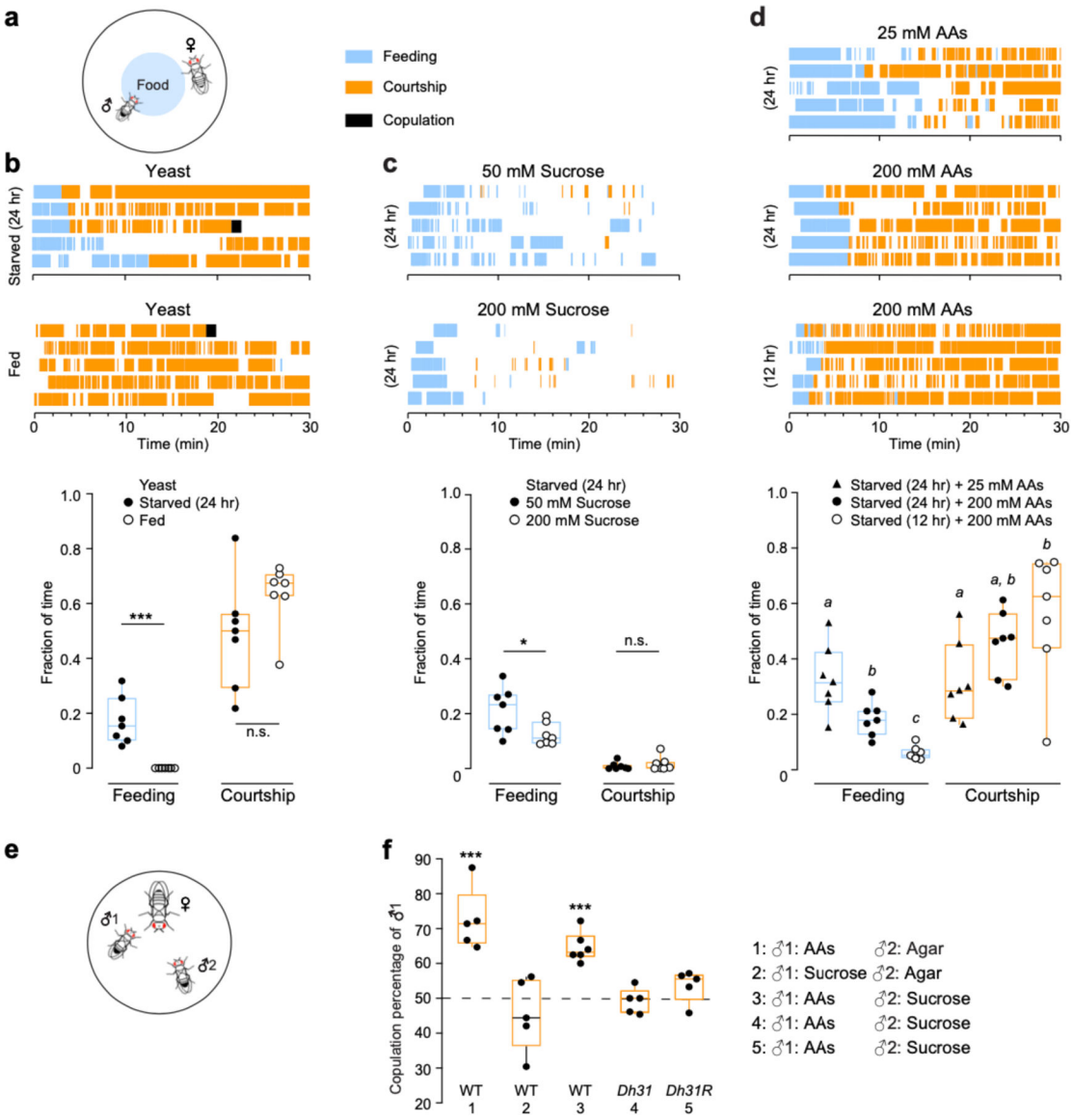

Figure 1. Consumption of amino acids suppresses feeding and promotes male courtship

(a) Simultaneous monitoring of feeding and courtship in individual males. One male was placed in a chamber with one virgin female and food. Behaviors were recorded for 30 min. (b-d) Effect of starvation duration and nutritional content on feeding and courtship behaviors. For each condition, the raster plots show the second-by-second behaviors of 5 representative males (top) and the fraction of time each male spent on feeding and courtship (bottom). n = 7 for each condition. n.s., not significant; *, $p < 0.05$; ***, $p < 0.001$; t-test (b and c) or different letters ($p<0.05$) as determined by ANOVA followed by Tukey's test (d). (e) A courtship competition assay with two naïve males and one WT virgin female. (f) Dh31 signaling is required for the effect of ingested amino acids on courtship. Two genetically identical males that were refed with different nutrients competed to copulate with one virgin female. Copulation percentages are shown for males fed on the indicated food source. Food sources: AAs, a mixture of all amino acids (total biologically available

nitrogen, 200 mM); sucrose, 50 mM; and agar. 5–6 experiments per condition and 18–25 successful matches per experiment. *p*-value was determined by Chi-square test. The dashed line indicates chance level. ***, $p < 0.001$.

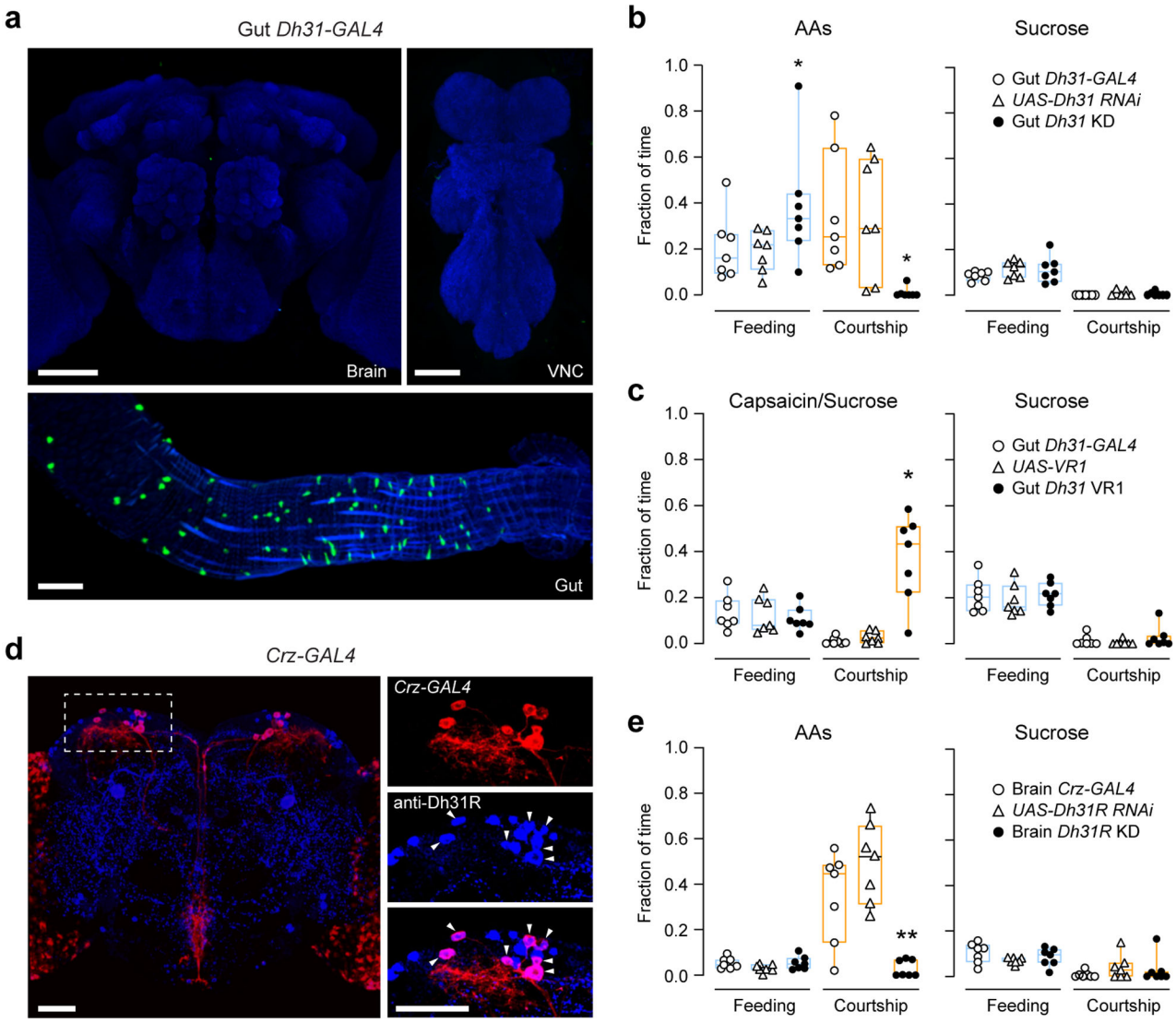

Figure 2. Gut Dh31 and brain Dh31R are required for the switch from feeding to courtship

(a) Dh31 enteroendocrine cells in the gut are specifically labeled by the combination of *Dh31-GAL4* and *Tsh-GAL80*. Images show the brain, VNC and gut of a fly containing *Dh31-GAL4*, *Tsh-GAL80* and UAS-CD8-GFP. Anti-GFP (green), nc82 in the brain and VNC (blue), phalloidin in the gut (blue).

(b) Gut-specific *Dh31* knockdown increased feeding duration and eliminated courtship when food contained amino acids (left) but had no effect when food contained only sucrose (right). GAL4: *Dh31-GAL4*, *Tsh-GAL80*. UAS: *UAS-Dh31-RNAi*. Gut *Dh31* KD flies had all three transgenes.

(c) Chemogenetic activation of gut *Dh31-GAL4* cells increased courtship duration. GAL4: *Dh31-GAL4*, *Tsh-GAL80*. UAS: *UAS-VR1*. Gut *Dh31* VR1 flies had all three transgenes.

(d) Confocal images show the expression pattern of *Crz-Gal4*. Samples were immuostained with anti-GFP (red) and anti-Dh31R (blue). Arrowheads indicate neurons that express both Dh31R and Crz.

(e) *Dh31R* knockdown in brain *Crz-GAL4* neurons eliminated the effect of amino acids on courtship. GAL4: *Crz-GAL4*, *tub>GAL80>stop*. UAS: *otd-nls::flp*, *UAS-Dh31R-RNAi*. Brain *Dh31R* KD flies had all four transgenes.

In (b, c, e), n = 7 for each genotype/condition. *, $p < 0.05$; **, $p < 0.01$; ANOVA followed by Tukey's test. Scale bar, 50 μm.

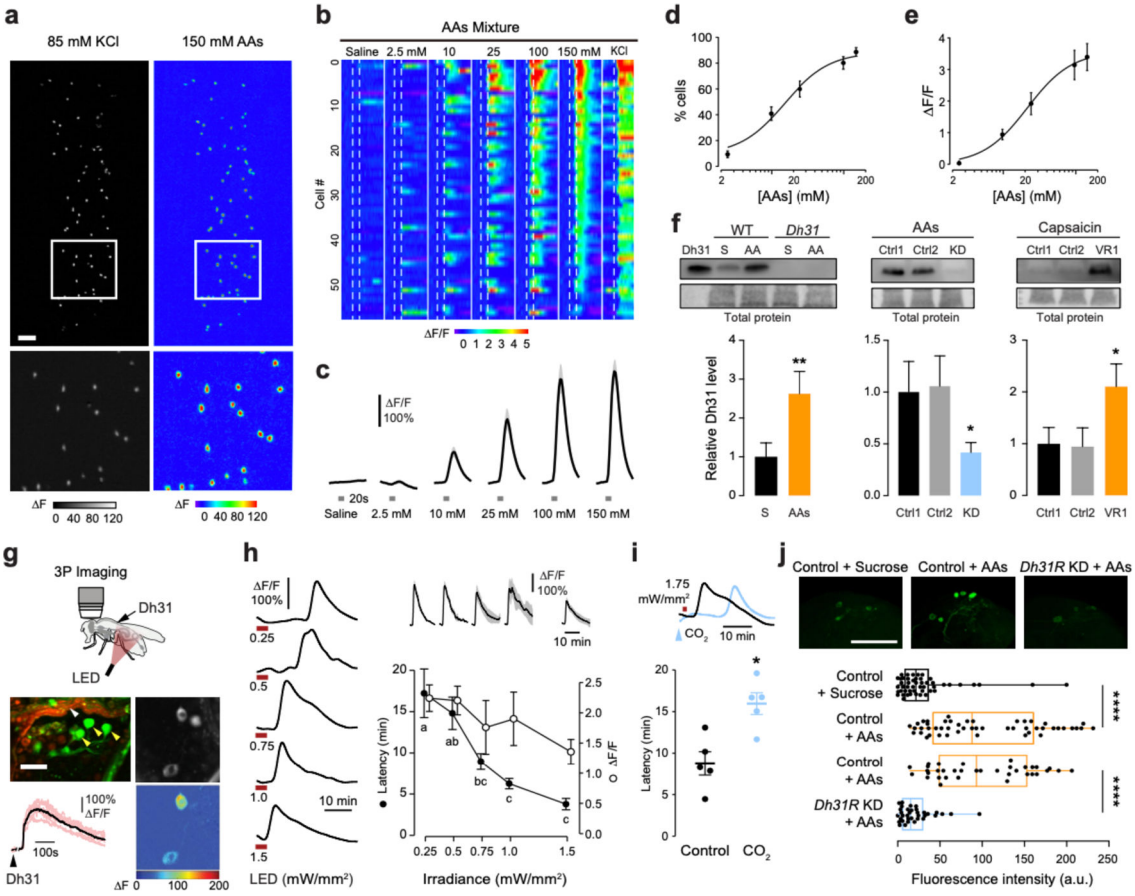

Figure 3. Dh31 released from the gut by amino acids activates Dh31R$^+$ neurons in the brain through circulation

(a) Amino acids evoked calcium response in Dh31$^+$ enteroendocrine cells. Grayscale image shows KCl-responsive Dh31$^+$ cells in posterior midgut and pseudocolored image shows amino acids-evoked responses in a representative sample. Scale bar, 50 μm.

(b) Response of individual Dh31$^+$ cells in a representative sample. Each row represents ΔF/F of one cell over time in response to different concentrations of amino acids. The vertical dash lines mark the beginning and end of stimulation.

(c) The average calcium response (ΔF/F) is shown in black with SEM as gray shaded areas (n=11). Gray lines below the traces indicate the stimulation period of amino acids or saline control.

(d) The percentage of responsive cells at different concentrations of amino acids.

(e) Dose-response curve of peak ΔF/F in response to amino acids from 2.5 to 150 mM.

(f) Hemolymph Dh31 levels in flies of various genotypes. Bar graphs show the relative Dh31 level normalized to control. Flies were starved for 24 hrs and then refed with different foods. Genotypes: WT; *Dh31* mutant; *Dh31* KD (*Dh31-GAL4*, *tsh-GAL80*, *UAS-Dh31 RNAi*); VR1 (*Dh31-GAL4*, *tsh-GAL80*, *UAS-VR1*). Foods: sucrose (50 mM), amino acids (200 mM) or capsaicin (50 μM mixed with 50 mM sucrose). Total protein was used as the loading control. 7 experiments per condition; 60 male flies per experiment. *, $p < 0.05$; **, $p < 0.01$. t-test or ANOVA followed by Tukey's test.

(g-i) Imaging calcium response of brain Crz^+ neurons with three-photon microscopy. Response of brain Crz^+ neurons to synthetic Dh31 peptide injected into the heart-tube of the fly. Image: three-photon fluorescence signals in green and third-harmonic signals in red. Scale bar, 25 μm. White arrow: cuticle; yellow arrows: Crz^+ neurons. Grayscale image shows GCaMP7s basal signal of Crz^+ neurons and pseudocolored image shows injection of Dh31-evoked response in a representative sample. The average calcium response (ΔF/F) is shown in black line with calcium response of individual flies shown in light red (n=6).
(h) Response of brain Crz^+ neurons to the activation of gut $Dh31^+$ cells. Latency and ΔF/F of Crz^+ neurons in response to optogenetic activation of gut $Dh31^+$ cells at stimulation intensity ranging from 0.25 to 1.5 mW/mm^2. Inset shows average ΔF/F traces aligned by the rising phase of each trace. n=7. Significant differences ($p < 0.05$) are indicated by different letters, ANOVA followed by Tukey's test.
(i) The effect of CO_2-induced cardiac arrest on the response latency of Crz^+ neurons in response to optogenetic activation of gut $Dh31^+$ cells. Stimulation intensity: 1.75 mW/mm^2. *, $p < 0.05$, n = 5, t-test.
(j) Expression of Dh31R in brain Crz^+ neurons is required for their increased calcium levels in response to ingested amino acids. Foods: sucrose (50 mM), AAs (200 mM). Flies: control (*Crz-GAL4*, *UAS-CaLexA*), *Dh31R* KD (*Crz-GAL4*, *UAS-CaLexA*, *UAS-Dh31R RNAi*). Confocal images show representative samples. Scale bar, 50 μm. Box plots show quantification of fluorescence intensity from Crz^+ neurons. 7 neurons per sample, 5–7 samples per condition. ****, $p < 0.0001$, Wilcoxon rank test. Error bars indicate SEM in all panels.

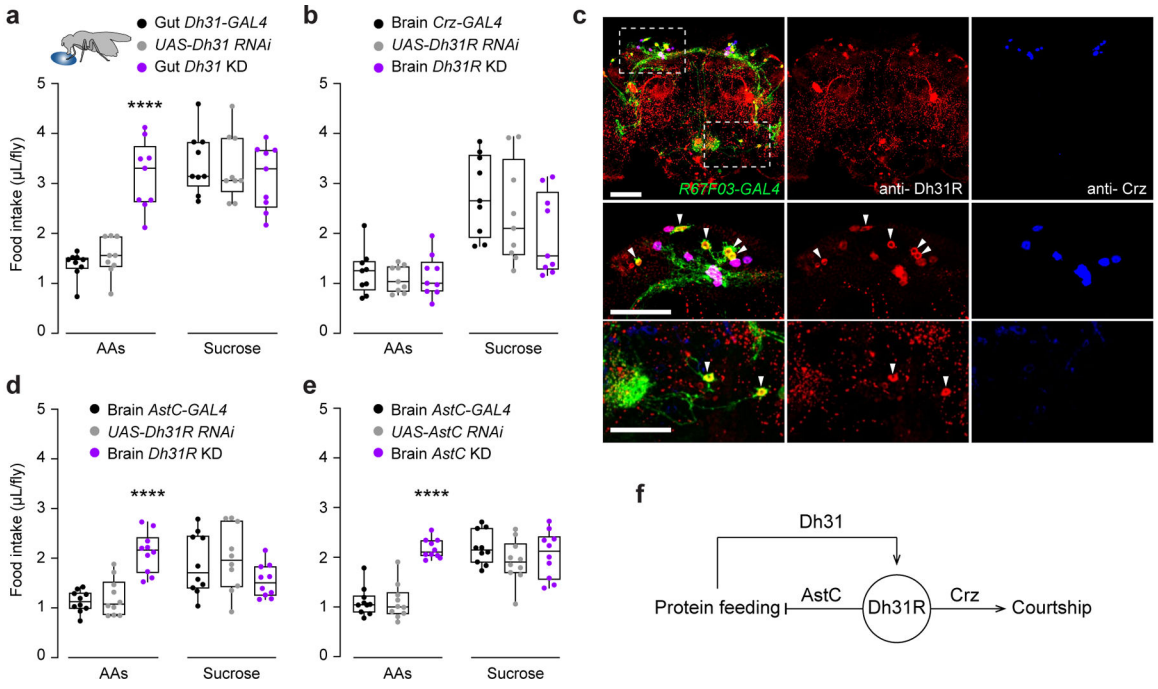

Figure 4. AstC release from a population of Dh31R^{+} neurons suppresses protein feeding

(a) Male flies with *Dh31* knockdown in the gut consumed more amino acids, but not sucrose, than controls.

(b) *Dh31R* knockdown in brain Crz^{+} neurons did not affect food intake.

(c) Confocal images show expression of GFP (green) in the brain of a male fly containing *R67F03-GAL4* and *UAS-CD8::GFP*. Anti-Dh31R (red) and anti-Crz (blue). Scale bar, 50 µm. Arrowheads indicate neurons positive for both Dh31R and AstC.

(d-e) Male flies with *Dh31R* (d) or *AstC* (e) knockdown in brain *R67F03* neurons consumed more amino acids, but not sucrose, than control flies. Brain *AstC-GAL4: R67F03-GAL4*, otd-nls::flp. *UAS-Dh31R RNAi*: *UAS-Dh31R-RNAi, tub>GAL80>stop*. Brain *Dh31R* KD flies have all four transgenes (d). Brain *AstC-GAL4*: *R67F03-GAL4*, *otd-nls::flp*. *UAS-AstC RNAi*: *UAS-AstC-RNAi, tub>GAL80>stop*. Brain *AstC* KD flies have all four transgenes (e).

(f) Model: gut derived neuropeptide Dh31 acts on brain neurons expressing Dh31R to regulate feeding and courtship behaviors through AstC and Crz, respectively.